European Journal of Control 58 (2021) 60–73

Contents lists available at ScienceDirect

European Journal of Control

journal homepage: www.elsevier.com/locate/ejcon

Reconstruction of admissible joint-references from a prescribed output-reference for the non-standard and generalized N-trailers

Maciej Marcin Michałek[a,*], Dariusz Pazderski[a]

Institute of Automatic Control and Robotics, Poznań University of Technology (PUT), Poznań, Poland

ARTICLE INFO

Article history:
Received 18 October 2019
Revised 22 October 2020
Accepted 20 November 2020
Available online 30 November 2020

Recommended by Prof. T Parisini

Keywords:
N-trailer kinematics
Inversion problem
Reference generator
On-axle/off-axle hitching
nSNT
GNT

ABSTRACT

A reconstruction of admissible reference signals for the inner dynamics upon a prescribed output reference of a dynamical system is a one of the key problems stated in the control theory. We address this problem with respect to a class of driftless dynamical systems representing nonholonomic kinematics of the N-trailers equipped with the on-axle and off-axle hitching, including difficult cases of the differentially non-flat and nonminimum-phase kinematics. Given a prescribed admissible reference path or trajectory for the last trailer's posture (treated as a reference output), we analyse possible solutions to the reconstruction problem for different types of the reference output. We propose a computational procedure to reconstruct the corresponding references (in a continuous domain of some parametrizing variable) for the joint angles of the N-trailer vehicles comprising an arbitrary number of segments interconnected by any type of hitching. In particular, we show how to find an *admissible* solution to the reconstruction problem, that is, the one which does not exhibit a jackknife effect, by appropriate searching in a set of all the possible (at least 2^N) solutions. The proposed computational method is formally explained and numerically verified for the 3-trailer kinematics equipped with various types of hitching.

1. Introduction

The problem of computing admissible reference signals for a dynamical system belongs to the fundamental and practically important issues addressed in the control theory. In the era of rapidly advancing development of automated and (semi-)autonomous articulated ground vehicles, in particular the so-called Large Capacity Vehicles or the N-trailer structures, the issue of finding the admissible reference configuration-trajectories (or paths) for this kind of systems in the context of various motion tasks becomes especially urgent today. In contrast to the so-called Standard N-Trailers (SNT), widely discussed in the literature [23,35], it turns out that the essential problem of reference signals computation has not been addressed with a sufficient attention thus far for the differentially non-flat Generalized N-Trailers (GNT) and non-Standard N-Trailers (nSNT), which contain the off-axle interconnections between trailers [2,15]. Due to the lack of a flatness property [35], and because of the nonminimum-phasiness of the angular kinematics [15], finding the admissible references for the nonholonomic GNT and nSNT structures is, in general, a difficult problem. In particular, we are interested in the *inversion problem*, [3,10,11], where for some *exosystem* $\dot{\boldsymbol{x}}_\Gamma = \boldsymbol{f}(\boldsymbol{x}_\Gamma, \boldsymbol{u}_\Gamma)$, with a reference state $\boldsymbol{x}_\Gamma \in \mathcal{Q}_x \subset \mathbb{R}^n$ and a reference input $\boldsymbol{u}_\Gamma \in \mathbb{R}^m$, and some prescribed output-reference $\boldsymbol{y}_\Gamma = \boldsymbol{h}(\boldsymbol{x}_\Gamma) \in \mathcal{Q}_y \subset \mathbb{R}^\chi$, $\chi < n$, we ask how to reconstruct the state-reference $\boldsymbol{x}_\Gamma$ and input $\boldsymbol{u}_\Gamma$ corresponding to the prescribed output-reference $\boldsymbol{y}_\Gamma$, simultaneously satisfying some additional admissibility conditions. This problem is especially important for the N-trailers, since most of the tasks defined for this kind of systems are determined first by the output-reference, prescribed for a selected (guidance) segment (e.g., for the last trailer or for a tractor), while the rest of reference state-variables and a reference control input for the vehicle must be reconstructed upon this output-reference.

The inversion problem is often related to the classical output tracking control task, which has been addressed for various types of dynamical systems, see [4,9–11,16,19,22,31,36,39]. However, for the differentially non-flat multi-body nonholonomic vehicles with unstable internal dynamics, see [15,18], it has not been addressed with a sufficient attention thus far. An origin of the inversion problem comes from the fact that in numerous applications only the output-reference is explicitly given a priori, either due to simplicity of the planning process (lower dimensionality, differential

* Corresponding author.
E-mail addresses: maciej.michalek@put.poznan.pl (M.M. Michałek), dariusz.pazderski@put.poznan.pl (D. Pazderski).

https://doi.org/10.1016/j.ejcon.2020.11.003

flatness, etc.), or due to a hierarchical nature of the control task where the output tracking is an essential control objective, while the state variables of the system shall only serve for this task. A similar situation holds for numerous practical motion problems defined for the N-trailers (see, e.g., [28]), where a primary objective is to guide only a distinguished vehicle's segment along a prescribed output-reference (e.g., a reference path/trajectory). Moreover, sometimes the output-reference is simply a recorded posture evolution of some other vehicle (even of a different kinematic structure relative to the considered N-trailer, like a single-body unicycle) which has to be followed by a selected segment of the N-trailer. In this case, there is no knowledge available about a required evolution of subordinate admissible joint-references and reference inputs for the N-trailer. Instead, they must be reconstructed solely upon the output-reference in a way to be *compatible* with N-trailer kinematics.

As a main contribution, we would like to complement the results available thus far for the differentially-flat SNT kinematics, by addressing a generic approach to the inversion problem applicable to any kinematics of the N-trailers with fixed (non-steerable) trailers' wheels, in particular, to the non-flat GNT and nSNT structures widely used in transportation. We provide the formulas of inverse velocity kinematics for both the off-axle and on-axle interconnections, which let one treat the inversion problem in a compact and coherent manner for various N-trailer structures. Furthermore, we show that a solution to the inversion problem for the N-trailers is not unique. Thus, finding an *admissible* solution to this problem (i.e., the one which avoids the jackknife phenomenon) is generally non-trivial. Next, we classify and discuss possible computational cases for the inversion problem in the context of N-trailers. Finally, we show that under some periodicity assumption, and for an output-reference predefined for the differentially-flat unicycle kinematics of the last trailer (an easy problem, [24,37]), it is possible to reconstruct the corresponding evolution of admissible reference joint-angles in the continuous-time domain for *any* differentially non-flat N-trailer kinematics by appropriately defining and solving a *curve-fitting*-like problem.

The paper is an extension of our prior conference work [29]. The main novel element added to the journal version comes from a derivation and usage of a new velocity transformation valid for the on-axle hitching, which has allowed extending the result from [29] to the GNT kinematics in a modular way. A presentation style of the current paper is more general relative to [29]. It makes the concept valid for both the reference trajectories and the reference paths. A more general way of a reliable selection of an initial condition (based on a homotopy concept) for the proposed iterative reconstruction algorithm, more advanced numerical examples given in the paper, and a detailed case-analysis provided for the 3-trailer kinematics equipped with a combination of the on- and off-axle hitching, all lead to a more deep insight into the considered reconstruction problem, and better illustrate the applicability range and computational effectiveness of the proposed iterative reconstruction method, which have not been possible to fully explore in [29]. To the authors' best knowledge, any systematic study of the joint-reference reconstruction problem for the N-trailers with arbitrary type of hitching has not been proposed in the literature thus far.

Notation In the text, we use a short notation $\mathrm{s}\alpha = \sin\alpha$ and $\mathrm{c}\alpha = \cos\alpha$; $\mathbb{T}^N$ denotes the N-dimensional torus; by $|\mathcal{S}|$ we denote a cardinality of set $\mathcal{S}$; the symbol $\triangleq$ means the equality by definition, while $:=$ is a substitution operator; two constant vectors, $\boldsymbol{c}^\top \triangleq [1\ 0]$ and $\boldsymbol{d}^\top \triangleq [0\ 1]$, will be used to simplify notation when manipulating with matrices and vectors; $p \in [0, \infty)$ denotes some parametrizing variable, while $(\cdot)'$ denotes a derivative with respect to p; a time derivative will be denoted by $\dot{(\cdot)}$. By $\|\cdot\|$ and $\|\cdot\|_\infty$ we denote, respectively, the 2-norm and ∞-norm of a vector. Since for the driftless dynamics a state is equivalent to a configuration, we will use the two terms interchangeably hereafter.

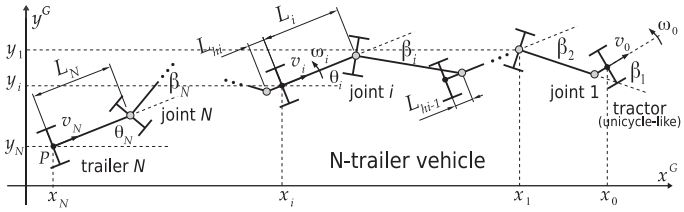

Fig. 1. Kinematic structure of the N-trailer with on-axle and off-axle hitching.

2. N-trailer kinematics

2.1. State vector and basic kinematic relationships

We will consider the N-trailer vehicles, which can be represented by the scheme in Fig. 1, comprising a unicycle-like tractor and an arbitrary number of N trailers with fixed (i.e., non-steerable) wheels. The trailers are indexed by the numbers $1, \ldots, N$, and the tractor is a segment indexed by 0. The trailers can be interconnected either by the on-axle or off-axle hitched passive rotary joints. Let us denote by $\mathcal{I}_{\mathrm{on}}$ and $\mathcal{I}_{\mathrm{off}}$ the sets of indexes corresponding, respectively, to the on-axle and off-axle hitched joints, such that $|\mathcal{I}_{\mathrm{on}}| + |\mathcal{I}_{\mathrm{off}}| = N$. Hereafter, we will be focusing on the two particular types of kinematic structures (see [15]): nSNT (non-Standard N-Trailers), characterized by the pair $(|\mathcal{I}_{\mathrm{on}}| = 0, |\mathcal{I}_{\mathrm{off}}| = N)$, and GNT (Generalized N-Trailers) corresponding to the pair $(0 < |\mathcal{I}_{\mathrm{on}}| < N, 0 < |\mathcal{I}_{\mathrm{off}}| < N)$. We distinguish two kinds of kinematic parameters: the trailer lengths $L_i > 0$, and the hitching offsets $L_{\mathrm{hi}} \in \mathbb{R}$, $i = 1, \ldots, N$, such that $|L_{\mathrm{hi}}| < L_i$ if $L_{\mathrm{hi}} < 0$ (a mechanical limitation). We also admit any possible combination of signs of the non-zero hitching offsets, that is, all positive (i.e., when the hitching points are located *behind* the preceding wheels' axles; cf. joint 1 in Fig. 1), all negative (i.e., when the hitching points are located *in front of* the preceding wheels' axles; cf. joint $i-1$ in Fig. 1), or mixed signs of offsets (positive and negative) in the same vehicle structure.

A configuration vector and a kinematic control input of the N-trailer can be described, respectively, by

$$\boldsymbol{q} \triangleq \begin{bmatrix} \boldsymbol{\beta} \\ \boldsymbol{q}_j \end{bmatrix} \in \mathbb{T}^N \times \mathbb{R}^3 \quad \text{and} \quad \boldsymbol{u}_0 = \begin{bmatrix} \omega_0 \\ v_0 \end{bmatrix} \in \mathbb{R}^2, \tag{1}$$

where $\boldsymbol{\beta} = [\beta_1\ \ \ldots\ \ \beta_N]^\top$ is a vector of joint-angles, which determines a vehicle *shape*, $\boldsymbol{q}_j = [\theta_j\ x_j\ y_j]^\top$, $j \in \{0, \ldots, N\}$, describes a posture of the distinguished segment (called the *guidance segment*), while ω_0 and v_0 are, respectively, the angular and longitudinal velocities of a tractor.

In the absence of a lateral skid in motion of all the vehicle's wheels, every ith vehicle segment can be treated as the kinematic unicycle

$$\dot{\boldsymbol{q}}_i = \boldsymbol{G}(\boldsymbol{q}_i)\boldsymbol{u}_i = \begin{bmatrix} 1 & 0 & 0 \\ 0 & \mathrm{c}\theta_i & \mathrm{s}\theta_i \end{bmatrix}^\top \begin{bmatrix} \omega_i \\ v_i \end{bmatrix}, \quad i = 0, \ldots, N \tag{2}$$

with the posture $\boldsymbol{q}_i = [\theta_i\ \ x_i\ \ y_i]^\top \in \mathbb{R}^3$ and the velocity $\boldsymbol{u}_i = [\omega_i\ v_i]^\top \in \mathbb{R}^2$. According to [15], and recalling that

$$\beta_i \triangleq \theta_{i-1} - \theta_i \quad \Rightarrow \quad \dot{\beta}_i = \omega_{i-1} - \omega_i, \tag{3}$$

where θ_i is an orientation of the ith vehicle's segment, a generic model of any N-trailer kinematics, with the guidance segment being the last trailer (i.e., by taking $j := N$), gets the form of a drift-

less system

$$\underbrace{\begin{bmatrix}\dot{\boldsymbol{\beta}}\\ \dot{\boldsymbol{q}}_N\end{bmatrix}}_{\dot{\boldsymbol{q}}} = \underbrace{\begin{bmatrix}\boldsymbol{S}_\beta(\boldsymbol{\beta})\\ \hline \boldsymbol{S}_N(\boldsymbol{\beta},\boldsymbol{q}_N)\end{bmatrix}}_{\boldsymbol{S}(\boldsymbol{q})}\boldsymbol{u}_0 = \begin{bmatrix}\boldsymbol{c}^\top\boldsymbol{\Gamma}_1(\beta_1)\\ \boldsymbol{c}^\top\boldsymbol{\Gamma}_2(\beta_2)\boldsymbol{J}_1(\beta_1)\\ \vdots\\ \boldsymbol{c}^\top\boldsymbol{\Gamma}_N(\beta_N)\boldsymbol{J}^1_{N-1}(\boldsymbol{\beta})\\ \hline \boldsymbol{G}(\boldsymbol{q}_N)\boldsymbol{J}^1_N(\boldsymbol{\beta})\end{bmatrix}\boldsymbol{u}_0, \tag{4}$$

where $\boldsymbol{\Gamma}_i(\beta_i) \triangleq \boldsymbol{I}_{2\times2} - \boldsymbol{J}_i(\beta_i)$, $\boldsymbol{I}_{2\times2} \in \mathbb{R}^{2\times2}$ is an identity matrix, $\boldsymbol{J}^1_i(\boldsymbol{\beta}) \triangleq \boldsymbol{J}_i(\beta_i)\ldots\boldsymbol{J}_1(\beta_1)$, while $\boldsymbol{J}_i(\beta_i)$ is a transformation matrix, the form of which will be explained in the next section. Selection $j := N$ is a special case but of practical importance, because in numerous practical motion tasks defined for the N-trailers the last segment plays a crucial role in guiding the whole articulated vehicle. As a consequence, and for the purposes of further considerations, let us complement (4) with an output equation

$$\boldsymbol{y} \triangleq \boldsymbol{q}_N = \underbrace{\begin{bmatrix}\boldsymbol{0}_{3\times N} & \boldsymbol{I}_{3\times3}\end{bmatrix}}_{\boldsymbol{C}}\boldsymbol{q}, \tag{5}$$

being a posture of the last trailer.

2.2. Forward velocity kinematics

One can easily check (see, e.g., [15]) that the matrix $\boldsymbol{J}_i(\beta_i)$, introduced in (4), maps the velocity $\boldsymbol{u}_{i-1}$ into $\boldsymbol{u}_i$ between any two neighbouring vehicle segments, that is,

$$\boldsymbol{u}_i = \underbrace{\begin{bmatrix}\frac{-L_{\mathrm{hi}}}{L_i}\mathrm{c}\beta_i & \frac{1}{L_i}\mathrm{s}\beta_i\\ L_{\mathrm{hi}}\mathrm{s}\beta_i & \mathrm{c}\beta_i\end{bmatrix}}_{\boldsymbol{J}_i(\beta_i)}\boldsymbol{u}_{i-1}. \tag{6}$$

By an iterative application of the above mapping, one derives the forward velocity kinematics

$$\boldsymbol{u}_i = \prod_{j=i}^{1}\boldsymbol{J}_j(\beta_j)\boldsymbol{u}_0 \quad \text{for} \quad i = 1,\ldots,N, \tag{7}$$

which is valid for any N-trailer structure, that is, with any number and any combination of the on-axle and/or off-axle interconnections.

2.3. Inverse velocity kinematics

The inverse velocity kinematics can be directly derived from (6) only for the nSNT structures, because the matrix $\boldsymbol{J}_i(\beta_i)$ is invertible for all β_i if $L_{\mathrm{hi}} \neq 0$. Namely,

$$\boldsymbol{u}_{i-1} = \underbrace{\begin{bmatrix}\frac{-L_i}{L_{\mathrm{hi}}}\mathrm{c}\beta_i & \frac{1}{L_{\mathrm{hi}}}\mathrm{s}\beta_i\\ L_i\mathrm{s}\beta_i & \mathrm{c}\beta_i\end{bmatrix}}_{\boldsymbol{J}_i^{-1}(\beta_i)}\boldsymbol{u}_i \quad \text{if} \quad i \in \mathcal{I}_{\mathrm{off}} \tag{8}$$

and, as a consequence,

$$\boldsymbol{u}_i = \prod_{j=i+1}^{N}\boldsymbol{J}_j^{-1}(\beta_j)\boldsymbol{u}_N \quad \text{for} \quad i = 0,\ldots,N-1. \tag{9}$$

However, if any jth trailer is on-axle hitched in a vehicle chain, then the corresponding matrix $\boldsymbol{J}_j(\beta_j)$ will be singular, and the inverse velocity kinematics (9) cannot be used. For this case, we propose to derive an alternative mapping between velocities of the neighbouring segments, which will allow us to address not only nSNT structures but also GNT kinematics, not considered in [29]. To this purpose, one can write upon (6), for $L_{\mathrm{hi}} = 0$, two equations valid for the on-axle hitching: $\omega_i = v_{i-1}\mathrm{s}\beta_i/L_i$ and $v_i = v_{i-1}\mathrm{c}\beta_i$. They lead to the following relations

$$v_{i-1} = \begin{bmatrix}L_i\mathrm{s}\beta_i & \mathrm{c}\beta_i\end{bmatrix}\boldsymbol{u}_i, \tag{10}$$

and

$$\beta_i = \beta_i^*, \quad \beta_i^* = \mathrm{Atan2}(\zeta_i L_i\omega_i, \zeta_i v_i), \tag{11}$$

where $\mathrm{Atan2}(\cdot,\cdot) : \mathbb{R}\times\mathbb{R} \to [-\pi,\pi)$ is a four-quadrant inverse-tangent function, $\zeta_i = \mathrm{sgn}(v_{i-1})$, whereas $\mathrm{sgn}(z) = +1$ if $z \geq 0$ and $\mathrm{sgn}(z) = -1$ otherwise. Computing a time-derivative of (11) gives

$$\dot{\beta}_i = \dot{\beta}_i^* = \frac{L_i v_i\dot{\omega}_i - L_i\omega_i\dot{v}_i}{v_i^2 + L_i^2\omega_i^2}, \tag{12}$$

which remains valid for $v_i^2 + L_i^2\omega_i^2 \neq 0$. By recalling (3), one can write

$$\begin{aligned}\omega_{i-1} &\overset{(3)}{=} \omega_i + \dot{\beta}_i \overset{(12)}{=} \omega_i + \frac{L_i v_i\dot{\omega}_i - L_i\omega_i\dot{v}_i}{v_i^2 + L_i^2\omega_i^2}\\ &= \left(1 + \frac{-L_i\dot{v}_i}{v_i^2 + L_i^2\omega_i^2}\right)\omega_i + \frac{L_i\dot{\omega}_i}{v_i^2 + L_i^2\omega_i^2}v_i\\ &= \begin{bmatrix}1 + \frac{-L_i\dot{v}_i}{v_i^2+L_i^2\omega_i^2} & \frac{L_i\dot{\omega}_i}{v_i^2+L_i^2\omega_i^2}\end{bmatrix}\begin{bmatrix}\omega_i\\ v_i\end{bmatrix}.\end{aligned} \tag{13}$$

Now, by collecting (13) and (10), one can write the following inverse velocity transformation for the on-axle hitching

$$\boldsymbol{u}_{i-1} = \underbrace{\begin{bmatrix}1 + \frac{-L_i\dot{v}_i}{v_i^2+L_i^2\omega_i^2} & \frac{L_i\dot{\omega}_i}{v_i^2+L_i^2\omega_i^2}\\ L_i\mathrm{s}\beta_i^* & \mathrm{c}\beta_i^*\end{bmatrix}}_{\boldsymbol{H}_i(\beta_i^*,\boldsymbol{u}_i,\dot{\boldsymbol{u}}_i)}\boldsymbol{u}_i \quad \text{if} \quad i \in \mathcal{I}_{\mathrm{on}}, \tag{14}$$

where β_i^* satisfies constraint (11), and matrix $\boldsymbol{H}_i(\beta_i^*,\boldsymbol{u}_i,\dot{\boldsymbol{u}}_i)$ explicitly depends on the (pseudo-)velocity $\boldsymbol{u}_i$ and (pseudo-)acceleration $\dot{\boldsymbol{u}}_i = [\dot{\omega}_i\ \dot{v}_i]^\top$.

Summarizing, upon the results (8) and (14), the inverse velocity kinematics for *any* N-trailer can be represented by the formula

$$\boldsymbol{u}_i = \prod_{j=i+1}^{N}\boldsymbol{P}_j(\beta_j,\boldsymbol{u}_j,\dot{\boldsymbol{u}}_j)\boldsymbol{u}_N \quad \text{for} \quad i = 0,\ldots,N-1, \tag{15}$$

where

$$\boldsymbol{P}_j(\beta_j,\boldsymbol{u}_j,\dot{\boldsymbol{u}}_j) := \begin{cases}\boldsymbol{J}_j^{-1}(\beta_j) & \text{if} \quad j \in \mathcal{I}_{\mathrm{off}}\\ \boldsymbol{H}_j(\beta_j^*,\boldsymbol{u}_j,\dot{\boldsymbol{u}}_j) & \text{if} \quad j \in \mathcal{I}_{\mathrm{on}}\end{cases}. \tag{16}$$

From now on, the matrices $\boldsymbol{P}_j(\beta_j,\boldsymbol{u}_j,\dot{\boldsymbol{u}}_j)$ will be used in the meaning resulting from substitution (16).

Remark 1. The velocity transformation (14) remains valid only for values of β_i satisfying constraint (11). This property will be important for the iterative solution to the reconstruction problem proposed in Section 4.3.2. The presence of the constraint (11) is a consequence of the differential flatness, locally preserved for a subsystem of two neighbouring vehicle's segments interconnected with the on-axle hitching. Furthermore, since $\beta_i = \beta_i^*(\boldsymbol{u}_i)$ in (11), up to the bi-valued factor $\zeta_i \in \{-1,+1\}$, the transformation matrix $\boldsymbol{H}_i(\beta_i^*(\boldsymbol{u}_i),\boldsymbol{u}_i,\dot{\boldsymbol{u}}_i) = \boldsymbol{H}_i(\boldsymbol{u}_i,\dot{\boldsymbol{u}}_i)$ essentially depends on the velocity and acceleration of the ith vehicle's segment. However, the notion $\boldsymbol{H}_i(\beta_i^*,\boldsymbol{u}_i,\dot{\boldsymbol{u}}_i)$ is useful in keeping a coherency and clear interpretation of our considerations, therefore it will be used in the rest of the paper.

Any derivative $\dot{\boldsymbol{u}}_i$ appearing in (16) can be ultimately expressed with appropriate derivatives of the velocity $\boldsymbol{u}_N$ by application of the following iterative formulas:

- if $(i+1) \in \mathcal{I}_{\mathrm{off}}$

$$\dot{\boldsymbol{u}}_i = \frac{\mathrm{d}\boldsymbol{J}_{i+1}^{-1}(\beta_{i+1})}{\mathrm{d}\beta_{i+1}}\dot{\beta}_{i+1}\boldsymbol{u}_{i+1} + \boldsymbol{J}_{i+1}^{-1}(\beta_{i+1})\dot{\boldsymbol{u}}_{i+1}, \tag{17}$$

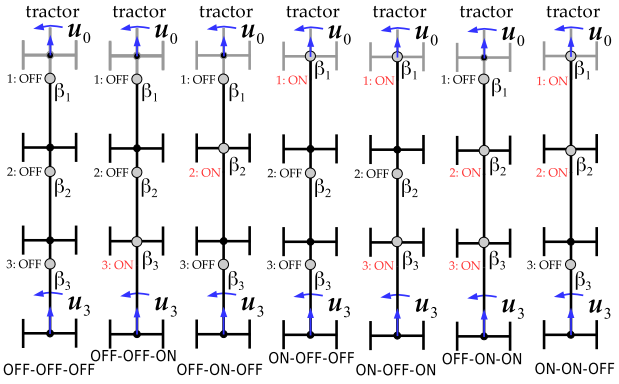

Fig. 2. Seven kinematic structures of the 3-trailers (nS3T and G3T) with various types of interconnections between the segments (only positive hitching offsets are shown for simplicity).

- if $(i+1) \in \mathcal{I}_{\text{on}}$

$$\dot{\boldsymbol{u}}_i = \frac{\mathrm{d}\boldsymbol{H}_{i+1}(\beta^*_{i+1}, \boldsymbol{u}_{i+1}, \dot{\boldsymbol{u}}_{i+1})}{\mathrm{d}t}\boldsymbol{u}_{i+1} + \boldsymbol{H}_{i+1}(\beta^*_{i+1}, \boldsymbol{u}_{i+1}, \dot{\boldsymbol{u}}_{i+1})\dot{\boldsymbol{u}}_{i+1}, \tag{18}$$

where for any $j \in \mathcal{I}_{\text{off}}$

$$\frac{\mathrm{d}\boldsymbol{J}_j^{-1}(\beta_j)}{\mathrm{d}\beta_j} = \begin{bmatrix} \frac{L_j}{L_{\text{hj}}}\mathrm{s}\beta_j & \frac{1}{L_{\text{hj}}}\mathrm{c}\beta_j \\ L_j\mathrm{c}\beta_j & -\mathrm{s}\beta_j \end{bmatrix}, \tag{19}$$

$$\dot{\beta}_j \overset{(3)}{=} \boldsymbol{c}^\top\left[\boldsymbol{J}_j^{-1}(\beta_j) - \boldsymbol{I}_{2\times 2}\right]\boldsymbol{u}_j, \tag{20}$$

while for any $j \in \mathcal{I}_{\text{on}}$

$$\frac{\mathrm{d}\boldsymbol{H}_j(\beta^*_j, \boldsymbol{u}_j, \dot{\boldsymbol{u}}_j)}{\mathrm{d}t} = \frac{\partial \boldsymbol{H}_j}{\partial \beta^*_j}\dot{\beta}^*_j + \frac{\partial \boldsymbol{H}_j}{\partial \omega_j}\dot{\omega}_j + \frac{\partial \boldsymbol{H}_j}{\partial v_j}\dot{v}_j + \frac{\partial \boldsymbol{H}_j}{\partial \dot{\omega}_j}\ddot{\omega}_j + \frac{\partial \boldsymbol{H}_j}{\partial \dot{v}_j}\ddot{v}_j, \tag{21}$$

$$\dot{\beta}^*_j = \frac{L_j v_j \dot{\omega}_j - L_j \omega_j \dot{v}_j}{v_j^2 + L_j^2\omega_j^2}. \tag{22}$$

The explicit forms of particular partial derivatives appearing in (21) are provided in Appendix A.

It is worth stressing that the formula (17) preserves a derivative-order for a velocity, that is, the left- and right-hand sides of (17) depend on the first-order derivatives of the velocities. On the other hand, the formula (18) does not preserve a derivative-order, because the term $\mathrm{d}\boldsymbol{H}/\mathrm{d}t$ depends on a velocity derivative of order two (see (21)). As a consequence, in the inverse velocity kinematics $\boldsymbol{u}_0 = \prod_{j=1}^{N}\boldsymbol{P}_j(\beta_j, \boldsymbol{u}_j, \dot{\boldsymbol{u}}_j)\boldsymbol{u}_N$, the right-hand side will depend only on the velocity $\boldsymbol{u}_N$ (but not on its derivatives) in the case of solely off-axle hitches, whereas every on-axle hitching will eventually introduce the dependence of the right-hand side of the inverse kinematics on a derivative of $\boldsymbol{u}_N$ of order increased by one.

2.4. Inverse velocity kinematics for the 3-trailers

General properties of the inverse velocity kinematics mentioned in Section 2.3 will be illustrated now by a case-study, in the form of seven examples (labelled as E1-E7), provided for the 3-trailer kinematics ($N = 3$) with various interconnections between the vehicle's segments[1] shown in Fig. 2. The case-study will allow us to formulate two practical corollaries at the end of this section.

[1] The notion, e.g., OFF-ON-ON denotes that the first joint is off-axle hitched, while the second and third ones are on-axle hitched in a vehicle kinematic chain.

E1: nS3T with the OFF-OFF-OFF hitching scheme leads to the inverse velocity kinematics

$$\boldsymbol{u}_0 = \boldsymbol{J}_1^{-1}(\beta_1)\boldsymbol{J}_2^{-1}(\beta_2)\boldsymbol{J}_3^{-1}(\beta_3)\boldsymbol{u}_3.$$

Thus, the right-hand side of the above formula depends in this case only on the velocity $\boldsymbol{u}_3$ thanks to the presence in a kinematic chain solely the off-axle hitching.

E2: G3T with the OFF-OFF-ON hitching scheme leads to the inverse velocity kinematics

$$\boldsymbol{u}_0 = \boldsymbol{J}_1^{-1}(\beta_1)\boldsymbol{J}_2^{-1}(\beta_2)\boldsymbol{H}_3(\beta^*_3, \boldsymbol{u}_3, \dot{\boldsymbol{u}}_3)\boldsymbol{u}_3.$$

where

$$\beta^*_3 \overset{(11)}{=} \mathrm{Atan2}(\zeta_3 L_3\omega_3, \zeta_3 v_3).$$

Thus, the right-hand side of the inverse kinematics depends in this case on the velocity $\boldsymbol{u}_3$ and on the acceleration $\dot{\boldsymbol{u}}_3$ due to a single on-axle hitching.

E3: G3T with the OFF-ON-OFF hitching scheme leads to the inverse velocity kinematics

$$\boldsymbol{u}_0 = \boldsymbol{J}_1^{-1}(\beta_1)\boldsymbol{H}_2(\beta^*_2, \boldsymbol{u}_2, \dot{\boldsymbol{u}}_2)\boldsymbol{J}_3^{-1}(\beta_3)\boldsymbol{u}_3,$$

where

$$\dot{\boldsymbol{u}}_2 = \frac{\mathrm{d}\boldsymbol{J}_3^{-1}}{\mathrm{d}\beta_3}\dot{\beta}_3\boldsymbol{u}_3 + \boldsymbol{J}_3^{-1}\dot{\boldsymbol{u}}_3,$$
$$\boldsymbol{u}_2 = \boldsymbol{J}_3^{-1}(\beta_3)\boldsymbol{u}_3,$$
$$\dot{\beta}_3 \overset{(20)}{=} \boldsymbol{c}^\top\left[\boldsymbol{J}_3^{-1}(\beta_3) - \boldsymbol{I}_{2\times 2}\right]\boldsymbol{u}_3,$$
$$\beta^*_2 \overset{(11)}{=} \mathrm{Atan2}(\zeta_2 L_2\omega_2, \zeta_2 v_2).$$

Thus, also in this case the right-hand side of the inverse kinematics depends on the velocity $\boldsymbol{u}_3$ and on the acceleration $\dot{\boldsymbol{u}}_3$ due to a single on-axle hitching (in spite of its different location in a vehicle chain relative to the example E2).

E4: G3T with the ON-OFF-OFF hitching scheme leads to the inverse velocity kinematics

$$\boldsymbol{u}_0 = \boldsymbol{H}_1(\beta^*_1, \boldsymbol{u}_1, \dot{\boldsymbol{u}}_1)\boldsymbol{J}_2^{-1}(\beta_2)\boldsymbol{J}_3^{-1}(\beta_3)\boldsymbol{u}_3,$$

where

$$\dot{\boldsymbol{u}}_1 = \frac{\mathrm{d}\boldsymbol{J}_2^{-1}}{\mathrm{d}\beta_2}\dot{\beta}_2\boldsymbol{J}_3^{-1}\boldsymbol{u}_3 + \boldsymbol{J}_2^{-1}\dot{\boldsymbol{u}}_2,$$
$$\dot{\boldsymbol{u}}_2 = \frac{\mathrm{d}\boldsymbol{J}_3^{-1}}{\mathrm{d}\beta_3}\dot{\beta}_3\boldsymbol{u}_3 + \boldsymbol{J}_3^{-1}\dot{\boldsymbol{u}}_3,$$
$$\boldsymbol{u}_1 = \boldsymbol{J}_2^{-1}\boldsymbol{J}_3^{-1}\boldsymbol{u}_3,$$
$$\dot{\beta}_2 = \boldsymbol{c}^\top\left[\boldsymbol{J}_2^{-1}(\beta_2) - \boldsymbol{I}_{2\times 2}\right]\boldsymbol{J}_3^{-1}\boldsymbol{u}_3,$$
$$\dot{\beta}_3 = \boldsymbol{c}^\top\left[\boldsymbol{J}_3^{-1}(\beta_3) - \boldsymbol{I}_{2\times 2}\right]\boldsymbol{u}_3,$$
$$\beta^*_1 \overset{(11)}{=} \mathrm{Atan2}(\zeta_1 L_1\omega_1, \zeta_1 v_1).$$

Also in this case the right-hand side of the inverse kinematics can be expressed with the velocity $\boldsymbol{u}_3$ and with the acceleration $\dot{\boldsymbol{u}}_3$ due to a single on-axle hitching (in spite of its different location in a vehicle chain relative to the examples E2 and E3).

E5: G3T with the ON-OFF-ON hitching scheme leads to the inverse velocity kinematics

$$\boldsymbol{u}_0 = \boldsymbol{H}_1(\beta^*_1, \boldsymbol{u}_1, \dot{\boldsymbol{u}}_1)\boldsymbol{J}_2^{-1}(\beta_2)\boldsymbol{H}_3(\beta^*_3, \boldsymbol{u}_3, \dot{\boldsymbol{u}}_3)\boldsymbol{u}_3,$$

where

$$\dot{\boldsymbol{u}}_1 = \frac{\mathrm{d}\boldsymbol{J}_2^{-1}}{\mathrm{d}\beta_2}\dot{\beta}_2\boldsymbol{H}_3\boldsymbol{u}_3 + \boldsymbol{J}_2^{-1}\dot{\boldsymbol{u}}_2,$$
$$\dot{\boldsymbol{u}}_2 = \dot{\boldsymbol{H}}_3\boldsymbol{u}_3 + \boldsymbol{H}_3\dot{\boldsymbol{u}}_3,$$
$$\dot{\beta}_2 = \boldsymbol{c}^\top\left[\boldsymbol{J}_2^{-1}(\beta_2) - \boldsymbol{I}_{2\times 2}\right]\boldsymbol{H}_3\boldsymbol{u}_3,$$

$$\boldsymbol{u}_1 = \boldsymbol{J}_2^{-1}\boldsymbol{H}_3\boldsymbol{u}_3,$$
$$\beta_j^* \overset{(11)}{=} \operatorname{Atan2}\big(\zeta_j L_j \omega_j, \zeta_j v_j\big), \quad j \in \{1,3\}.$$

Since $\dot{\boldsymbol{H}}_3$ depends on $\ddot{\boldsymbol{u}}_3$ (cf. (21)), the right-hand side of the inverse kinematics depends in this case on the velocity $\boldsymbol{u}_3$, on the acceleration $\dot{\boldsymbol{u}}_3$, and on the jerk $\ddot{\boldsymbol{u}}_3$ due to the double on-axle hitching present in the kinematic chain.

E6: G3T with the OFF-ON-ON hitching scheme leads to the inverse velocity kinematics

$$\boldsymbol{u}_0 = \boldsymbol{J}_1^{-1}(\beta_1)\boldsymbol{H}_2(\beta_2^*, \boldsymbol{u}_2, \dot{\boldsymbol{u}}_2)\boldsymbol{H}_3(\beta_3^*, \boldsymbol{u}_3, \dot{\boldsymbol{u}}_3)\boldsymbol{u}_3,$$

where

$$\dot{\boldsymbol{u}}_2 = \dot{\boldsymbol{H}}_3\,\boldsymbol{u}_3 + \boldsymbol{H}_3\dot{\boldsymbol{u}}_3,$$
$$\boldsymbol{u}_2 = \boldsymbol{H}_3\boldsymbol{u}_3,$$
$$\beta_j^* \overset{(11)}{=} \operatorname{Atan2}\big(\zeta_j L_j \omega_j, \zeta_j v_j\big), \quad j \in \{2,3\}.$$

Since $\dot{\boldsymbol{H}}_3$ depends on $\ddot{\boldsymbol{u}}_3$ (cf. (21)), the right-hand side of the inverse kinematics depends on the velocity $\boldsymbol{u}_3$, on the acceleration $\dot{\boldsymbol{u}}_3$, and on the jerk $\ddot{\boldsymbol{u}}_3$ due to the double on-axle hitching present in the kinematic chain.

E7: G3T with the ON-ON-OFF hitching scheme leads to the inverse velocity kinematics

$$\boldsymbol{u}_0 = \boldsymbol{H}_1(\beta_1^*, \boldsymbol{u}_1, \dot{\boldsymbol{u}}_1)\boldsymbol{H}_2(\beta_2^*, \boldsymbol{u}_2, \dot{\boldsymbol{u}}_2)\boldsymbol{J}_3^{-1}(\beta_3)\boldsymbol{u}_3,$$

where

$$\dot{\boldsymbol{u}}_1 = \dot{\boldsymbol{H}}_2\,\boldsymbol{u}_2 + \boldsymbol{H}_2\dot{\boldsymbol{u}}_2,$$
$$\boldsymbol{u}_1 = \boldsymbol{H}_2\boldsymbol{J}_3^{-1}\boldsymbol{u}_3,$$
$$\dot{\boldsymbol{u}}_2 = \frac{d\boldsymbol{J}_3^{-1}}{d\beta_3}\dot{\beta}_3\,\boldsymbol{u}_3 + \boldsymbol{J}_3^{-1}\dot{\boldsymbol{u}}_3,$$
$$\boldsymbol{u}_2 = \boldsymbol{J}_3^{-1}\boldsymbol{u}_3,$$
$$\dot{\beta}_3 = \boldsymbol{c}^\top\big[\boldsymbol{J}_3^{-1}(\beta_3) - \boldsymbol{I}_{2\times 2}\big]\boldsymbol{u}_3,$$
$$\beta_j^* \overset{(11)}{=} \operatorname{Atan2}\big(\zeta_j L_j \omega_j, \zeta_j v_j\big), \quad j \in \{1,2\}.$$

Because the term $\dot{\boldsymbol{H}}_2$ depends on (see (21))

$$\ddot{\boldsymbol{u}}_2 = \left[\frac{\mathrm{d}^2\boldsymbol{J}_3^{-1}}{\mathrm{d}\beta_3^2}\dot{\beta}_3 + \frac{\mathrm{d}\boldsymbol{J}_3^{-1}}{\mathrm{d}\beta_3}\ddot{\beta}_3\right]\boldsymbol{u}_3 + 2\frac{\mathrm{d}\boldsymbol{J}_3^{-1}}{\mathrm{d}\beta_3}\dot{\beta}_3\dot{\boldsymbol{u}}_3 + \boldsymbol{J}_3^{-1}\ddot{\boldsymbol{u}}_3,$$

and since

$$\ddot{\beta}_3 \overset{(20)}{=} \boldsymbol{c}^\top\left(\frac{d\boldsymbol{J}_3^{-1}}{d\beta_3}\dot{\beta}_3\boldsymbol{u}_3 + \big[\boldsymbol{J}_3^{-1} - \boldsymbol{I}_{2\times 2}\big]\dot{\boldsymbol{u}}_3\right),$$

the right-hand side of the inverse kinematics depends in this case on the velocity $\boldsymbol{u}_3$, on the acceleration $\dot{\boldsymbol{u}}_3$, and on the jerk $\ddot{\boldsymbol{u}}_3$ due to the double on-axle hitching (despite their different location in a vehicle chain relative to the example E6).

The above examples allow formulating the following.

Corollary 1. *The presence of any on-axle hitching in the N-trailer kinematics imposes an additional smoothness requirement on a trajectory of the last trailer – the inverse velocity kinematics additionally depends on a higher-order derivative of velocity $\boldsymbol{u}_N$. Every on-axle hitching increases the derivative-order by one, leading to the dependence of $\boldsymbol{u}_0$ on derivatives $\boldsymbol{u}_N^{(\eta)}$, up to the order $\eta = |\mathcal{I}_{\mathrm{on}}|$.*

Corollary 2. *A location of the on-axle hitching in a kinematic chain does not affect Corollary 1. However, the location of the on-axle hitching closer to the tractor segment (in a vehicle chain) makes computations of the inverse velocity kinematics more complex (cf., e.g., examples E2 with E3 and E4).*

Remark 2. Although the paper does not address directly the SNT kinematics (which is a differentially flat system, [34]), the inverse velocity kinematics for this type of vehicles can be computed as $\boldsymbol{u}_0 = \boldsymbol{H}_1(\beta_1^*, \boldsymbol{u}_1, \dot{\boldsymbol{u}}_1)\boldsymbol{H}_2(\beta_2^*, \boldsymbol{u}_2, \dot{\boldsymbol{u}}_2)\boldsymbol{H}_3(\beta_3^*, \boldsymbol{u}_3, \dot{\boldsymbol{u}}_3)\boldsymbol{u}_3$, where velocities $\boldsymbol{u}_1$, $\boldsymbol{u}_2$, and derivatives $\dot{\boldsymbol{u}}_1$, $\dot{\boldsymbol{u}}_2$, can be eventually expressed with $\boldsymbol{u}_3$ and its derivatives up to the order of 3 in this case. Note that the joint angles β_1^*, β_2^*, and β_3^* used in matrices $\boldsymbol{H}_i$, $i = 1,2,3$, have to satisfy constraint (11), like in the case of all matrices $\boldsymbol{H}_i$ used in the examples E2 to E7 above.

3. Admissible state-references for the N-trailers

In order to make the forthcoming considerations general enough (taking into account both the reference paths and trajectories), let $p \in \mathbb{R}$ be some parametrizing variable which can be interpreted as time ($p \equiv t$, $z(p) \equiv z(t) \;\Rightarrow\; \dot{z}(t) \equiv z'(p)$), scaled time ($p = \alpha t$ for $\alpha > 0$, $z(p) \;\Rightarrow\; \dot{z}(t) = \alpha z'(p)$), or a (signed) curvilinear length of a geometrical path ($z(p) \;\Rightarrow\; \dot{z}(t) = z'(p)\mathrm{d}p/\mathrm{d}t$).

3.1. Problem formulation

Let us divide the state-reference

$$\boldsymbol{q}_{\mathrm{r}}(p) \triangleq [\boldsymbol{\beta}_{\mathrm{r}}^\top(p)\ \boldsymbol{q}_{N\mathrm{r}}^\top(p)]^\top \in \mathbb{T}^N \times \mathbb{R}^3 \tag{23}$$

into the *joint-reference* (or *shape-reference*) $\boldsymbol{\beta}_{\mathrm{r}}(p)$ and the *guidance-reference* $\boldsymbol{q}_{N\mathrm{r}}(p)$. Following [11], we formulate a general inversion problem for the N-trailers.

Problem 1 (Inversion problem for the N-trailers)**.** For a prescribed output-reference (being a guidance-reference)

$$\boldsymbol{y}_{\mathrm{r}}(p) \overset{(5)}{=} \boldsymbol{q}_{N\mathrm{r}}(p) = \boldsymbol{C}\boldsymbol{q}_{\mathrm{r}}(p) \tag{24}$$

find a bounded state-reference $\boldsymbol{q}_{\mathrm{r}}(p)$ and a bounded reference input $\boldsymbol{u}_{0\mathrm{r}}(p)$ which satisfy dynamics of the exosystem

$$\boldsymbol{q}_{\mathrm{r}}'(p) = \begin{bmatrix}\boldsymbol{\beta}_{\mathrm{r}}'(p)\\ \boldsymbol{q}_{N\mathrm{r}}'(p)\end{bmatrix} = \boldsymbol{S}(\boldsymbol{q}_{\mathrm{r}}(p))\boldsymbol{u}_{0\mathrm{r}}(p), \tag{25}$$

where the form of matrix $\boldsymbol{S}(\boldsymbol{q}_{\mathrm{r}}(p))$ results from (4).

In the above formulation we have not imposed yet any additional admissibility conditions for $\boldsymbol{q}_{\mathrm{r}}(p)$ – they will be addressed in Sections 3.2 and 3.3.

Remark 3. Planning the guidance-reference (24) for the differentially flat unicycle-like kinematics (2) of the guidance segment is a classical and relatively easy problem (see, e.g., [30,37] and references therein). It is much easier when compared to planning of the whole state-reference $\boldsymbol{q}_{\mathrm{r}}(p)$ together with the reference input $\boldsymbol{u}_{0\mathrm{r}}(p)$ for the multi-body nonholonomic vehicles like N-trailers (as addressed, e.g., in [13,25,26]). The above arguments lead to the main motivation for the above decomposition of the reference signals, characteristic to the inversion problem.

It is useful to rewrite (25) in another form to better reflect the above mentioned hierarchical formulation of the reference evolution for the N-trailer configuration. By recalling the inverse kinematics (15) one may write

$$\boldsymbol{u}_{0\mathrm{r}}(p) = \prod_{j=1}^{N}\boldsymbol{P}_j(\beta_{j\mathrm{r}}(p), \boldsymbol{u}_{j\mathrm{r}}(p), \dot{\boldsymbol{u}}_{j\mathrm{r}}(p))\boldsymbol{u}_{N\mathrm{r}}(p), \tag{26}$$

and, as a consequence, (omitting the argument p for compactness)

$$\begin{bmatrix}\boldsymbol{\beta}_{\mathrm{r}}'\\ \boldsymbol{q}_{N\mathrm{r}}'\end{bmatrix} \overset{(25)}{=} \boldsymbol{S}(\boldsymbol{q}_{\mathrm{r}})\prod_{j=1}^{N}\boldsymbol{P}_j(\beta_{j\mathrm{r}}, \boldsymbol{u}_{j\mathrm{r}}, \boldsymbol{u}_{j\mathrm{r}}')\boldsymbol{u}_{N\mathrm{r}}$$

$$\overset{(4)}{=} \begin{bmatrix} \boldsymbol{S}_\beta(\boldsymbol{\beta}_\Gamma) \prod_{j=1}^{N} \boldsymbol{P}_j(\beta_{j\Gamma}, \boldsymbol{u}_{j\Gamma}, \boldsymbol{u}'_{j\Gamma}) \\ \boldsymbol{G}(\boldsymbol{q}_{N\Gamma}) \end{bmatrix} \boldsymbol{u}_{N\Gamma}, \tag{27}$$

where a form of the matrix $\boldsymbol{G}$ results from (2), $\boldsymbol{u}_{N\Gamma}(p) = [\omega_{N\Gamma}(p)\ \ v_{N\Gamma}(p)]^\top \in \mathbb{R}^2$ is a *reference guiding* velocity prescribed along $\boldsymbol{q}_{N\Gamma}(p)$, and (cf. (16))

$$\boldsymbol{P}_j(\beta_{j\Gamma}, \boldsymbol{u}_{j\Gamma}, \boldsymbol{u}'_{j\Gamma}) := \begin{cases} \boldsymbol{J}_j^{-1}(\beta_{j\Gamma}) & \text{if} \quad j \in \mathcal{I}_{\text{off}} \\ \boldsymbol{H}_j(\beta^*_{j\Gamma}, \boldsymbol{u}_{j\Gamma}, \boldsymbol{u}'_{j\Gamma}) & \text{if} \quad j \in \mathcal{I}_{\text{on}} \end{cases}, \tag{28}$$

with

$$\beta^*_{j\Gamma} \triangleq \left\{ \beta_{j\Gamma} : \beta_{j\Gamma} \overset{(11)}{=} \text{Atan2}\big(\zeta_\Gamma L_j \omega_{j\Gamma}, \zeta_\Gamma v_{j\Gamma}\big) \right\}, \tag{29}$$

where $\zeta_\Gamma = \text{sgn}(v_{\lfloor j-1 \rfloor \Gamma})$. Since every vehicle segment is described by the unicycle kinematics (2), the output-reference $\boldsymbol{q}_{N\Gamma}(p)$ and the reference guiding velocity $\boldsymbol{u}_{N\Gamma}(p)$ must be related with the unicycle kinematics too (see Section 3.2).

Remark 4. By analogy to (17) and (18), any derivative $\boldsymbol{u}'_{i\Gamma}(p)$ appearing in (28) can be ultimately expressed by combinations of the reference guiding velocity $\boldsymbol{u}_{N\Gamma}(p)$ and its derivatives with respect to p, up to the appropriate order (i.e., by $\boldsymbol{u}'_{N\Gamma}(p)$, $\boldsymbol{u}''_{N\Gamma}(p)$,...,$\boldsymbol{u}^{(\eta)}_{N\Gamma}(p)$).

Upon (26) and (27) it is evident now that solving the Problem 1 reduces to finding the joint-reference $\boldsymbol{\beta}_\Gamma(p)$.

3.2. Admissible guidance-reference

We assume that the guidance-reference

$$\boldsymbol{q}_{N\Gamma}(p) = [\theta_{N\Gamma}(p)\ x_{N\Gamma}(p)\ y_{N\Gamma}(p)]^\top \in \mathbb{R}^3 \tag{30}$$

satisfies the following admissibility conditions:

C1. $\forall\, p \in \mathbb{R} \quad \boldsymbol{q}'_{N\Gamma}(p) = \boldsymbol{G}(\boldsymbol{q}_{N\Gamma}(p))\boldsymbol{u}_{N\Gamma}(p)$,
C2. $\forall\, p \in \mathbb{R} \quad \|\boldsymbol{u}_{N\Gamma}(p)\| < \infty$ and $v_{N\Gamma}(p_1)v_{N\Gamma}(p_2) > 0$ for all $p_1, p_2 \in \mathbb{R}$,
C3. $\boldsymbol{u}_{N\Gamma}(p) \in \mathcal{C}^\eta$, $\eta \geq \max\{1, |\mathcal{I}_{\text{on}}|\}$.

Condition C1 (as a consequence of (27)) guarantees satisfaction of nonholonomic constraints of the unicycle-like kinematics (2). Hence, the dynamics used in condition C1 may be treated as an exosystem for the output-reference. C2 imposes an upper bound on the reference guiding velocity, and also ensures satisfaction of the particular *persistent excitation* condition for the guidance-reference (30), according to which the reference guidance segment moves along $\boldsymbol{q}_{N\Gamma}(p)$ with a non-zero longitudinal velocity $v_{N\Gamma}(p)$ of a constant sign (that is, only forward or only backward). Condition C3 forces some minimal degree of smoothness (strictly: continuity of degree η) for the reference guiding velocity along $\boldsymbol{q}_{N\Gamma}(p)$, which directly comes from Corollary 1, and is required to ensure boundedness of the matrices $\boldsymbol{H}_j$ used in (26)–(28) for the on-axle hitches. According to the above conditions, the guidance-reference (30) can be any sufficiently smooth and persistently exciting reference which is feasible for the unicycle kinematics.

3.3. Admissible joint-reference

According to (27), one observes that an admissible joint-reference $\boldsymbol{\beta}_\Gamma(p)$ is related with the guidance-reference $\boldsymbol{q}_{N\Gamma}(p)$ through the reference guiding velocity $\boldsymbol{u}_{N\Gamma}(p)$ satisfying dynamics of the joint-reference exosystem

$$\boldsymbol{\beta}'_\Gamma(p) = \boldsymbol{S}_\beta(\boldsymbol{\beta}_\Gamma(p)) \prod_{j=1}^{N} \boldsymbol{P}_j(\beta_{j\Gamma}(p), \boldsymbol{u}_{j\Gamma}(p), \boldsymbol{u}'_{j\Gamma}(p))\boldsymbol{u}_{N\Gamma}(p). \tag{31}$$

Thus, any joint-reference corresponding to the guidance-reference (30) must be a solution of (31).

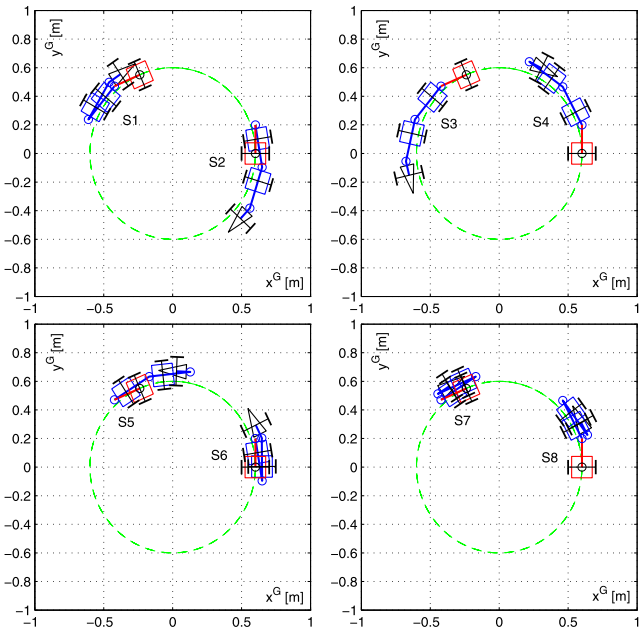

Fig. 3. Graphical illustration of $2^3 = 8$ possible sets (denoted by S1 to S8) of the reference joint-angles for the nS3T kinematics corresponding to the same circular guidance-reference (the guidance segment has been highlighted in red).

Since the kinematics (27) can be a differentially non-flat system, see [2,35], it is unknown in general (except the simplest cases) how to find an admissible joint-reference $\boldsymbol{\beta}_\Gamma(p) = [\beta_{1\Gamma}(p) \dots \beta_{N\Gamma}(p)]^\top \in \mathbb{T}^N$, corresponding to the admissible guidance-reference (30), in a closed form. Moreover, in practical applications we usually want to avoid the so-called *jackknife effect* corresponding to the vehicle folding in the joints. Therefore, avoidance of a jackknife effect should be imposed on the joint-reference $\boldsymbol{\beta}_\Gamma(p)$ as an additional admissibility condition for a solution to Problem 1. Because the jackknife effect is explained in various ways in the literature of the N-trailers, we propose (following [27]) to formulate the *anti-jackknife* admissibility condition in the form

C4. $\forall\, \boldsymbol{\beta}_\Gamma \quad v_{\lfloor i-1 \rfloor \Gamma}(\boldsymbol{\beta}_\Gamma(p), \boldsymbol{u}_{N\Gamma}(p)) \cdot v_{i\Gamma}(\boldsymbol{\beta}_\Gamma(p), \boldsymbol{u}_{N\Gamma}(p)) > 0$ for all $i = 1, \dots, N$,

where $v_{i\Gamma}(\boldsymbol{\beta}_\Gamma, \boldsymbol{u}_{N\Gamma}) = \boldsymbol{d}^\top \prod_{j=i+1}^{N} \boldsymbol{P}_j(\beta_{j\Gamma}, \boldsymbol{u}_{j\Gamma}, \boldsymbol{u}'_{j\Gamma})\boldsymbol{u}_{N\Gamma}$ is a reference longitudinal velocity for the ith vehicle's segment. A physical interpretation of condition C4 is clear and general (cf. also [29]) – it admits only those joint-references which lead to the same constant signs of the reference longitudinal velocities for all the vehicle's segments. Thus, under condition C4, the sign $\zeta_\Gamma = \text{sgn}(v_{\lfloor j-1 \rfloor \Gamma})$ used in (29) can be uniquely determined upon the prescribed reference guidance velocity by setting $\zeta_r := \text{sgn}(v_{N\Gamma})$. Following [27], let us call all the state-references $\boldsymbol{q}_\Gamma(p)$ satisfying C4 as the *Segment-Platooning* (S-P) references, since along any such admissible reference all the segments of a reference N-trailer move like in a platoon formation.

In Section 4, we reveal that a solution of Eq. (31) is not unique. It means that there exist multiple solutions of (31), all corresponding to the same guidance-reference $\boldsymbol{q}_{N\Gamma}(p)$. To be more specific, Fig. 3 illustrates eight different solutions (denoted by S1 to S8), obtained for the nS3T kinematics, which correspond to the same circular guidance-reference of radius $R_r = 0.6$ m and of a constant reference guiding velocity $\boldsymbol{u}_{N\Gamma}$. The solutions differ from each other by satisfaction or violation of the anti-jackknife admissibility condition. Note that only the set S3 satisfies the admissibility condition C4 preventing the occurrence of the jackknife effect. A

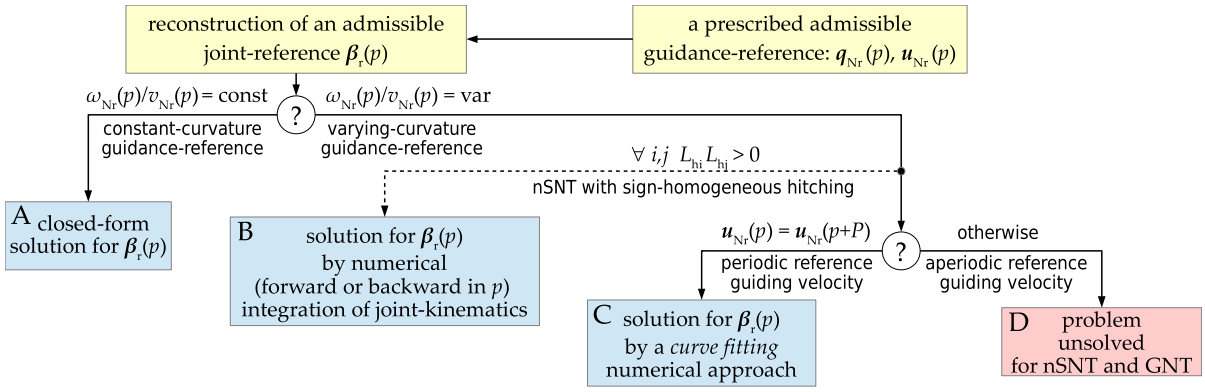

Fig. 4. A classification of computational approaches to a reconstruction of the admissible joint-reference for the nSNT and GNT kinematics for various characteristics of the reference guiding velocity $\boldsymbol{u}_{N\mathrm{r}}$ and the hitching offsets L_{h}.

number of solutions compatible with the same guidance-reference $\boldsymbol{q}_{N\mathrm{r}}(p)$ comes from a number of trailers, and in this case equals $2^3 = 8$. The solutions result from two possible types of motion for every ith joint: the one satisfying C4, and the other one violating C4. This non-uniqueness additionally aggravates the problem of reconstructing an admissible joint-reference $\boldsymbol{\beta}_{\mathrm{r}}(p)$ by a necessity of finding only this one which respects C4.

Remark 5. In order to make the forthcoming considerations meaningful, we need to assume that the guidance-reference (30), satisfying C1-C3, is such that there exists at least one (a priori unknown) solution $\breve{\boldsymbol{\beta}}_{\mathrm{r}}(p)$ of (31) leading to the state-reference $\boldsymbol{q}_{\mathrm{r}}(p) = [\breve{\boldsymbol{\beta}}_{\mathrm{r}}^{\top}(p)\ \boldsymbol{q}_{N\mathrm{r}}^{\top}(p)]^{\top}$ of the S-P type. This is the underlying existence assumption.

4. Reconstruction of admissible joint-references

4.1. General classification of computational cases

The scheme presented in Fig. 4 explains four possible computational approaches to the reconstruction problem denoted as cases A to D.

We will address or comment all the cases in the forthcoming subsections. A numerical algorithm corresponding to the case C in Fig. 4 belongs to the main result of the paper.

4.2. Reconstruction for the constant-curvature guidance-references

This is the simplest situation (denoted as case A in Fig. 4) where the guidance-reference $\boldsymbol{q}_{N\mathrm{r}}(p)$ corresponds to the rectilinear or circular (i.e., constant-curvature) motion of the guidance segment, that is, when $\omega_{N\mathrm{r}}(p)/v_{N\mathrm{r}}(p) = \text{const}$ for all $p \in \mathbb{R}$. In this case there exists a closed-form solution to dynamics (31), see [8,15,29]. Namely, the admissible joint-references $\beta_{i\mathrm{r}}$ (which are constant in these conditions) satisfying C1 to C4 can be computed for $i \in \{1, \ldots, N\}$ as follows:

$$\beta_{i\mathrm{r}} = \begin{cases} 0 & \text{if} \quad \omega_{N\mathrm{r}} \equiv 0 \\ \mathrm{Atan2}(z_{1i}, z_{2i}) & \text{if} \quad \omega_{N\mathrm{r}} \not\equiv 0 \end{cases}, \tag{32}$$

where

$$z_{1i} = L_i R_{[i-1]\mathrm{r}} + L_{\mathrm{h}i} R_{i\mathrm{r}}, \tag{33}$$

$$z_{2i} = R_{i\mathrm{r}} R_{[i-1]\mathrm{r}} - L_i L_{\mathrm{h}i}, \tag{34}$$

$$R_{N\mathrm{r}} \triangleq v_{N\mathrm{r}}(p)/\omega_{N\mathrm{r}}(p) = \text{const}, \tag{35}$$

$$R_{[i-1]\mathrm{r}} = \xi_{i-1}\sqrt{R_{i\mathrm{r}}^2 + L_i^2 - L_{\mathrm{h}i}^2}, \tag{36}$$

$$\xi_{i-1} = \mathrm{sgn}(R_{N\mathrm{r}}), \tag{37}$$

whereas $\xi_{i-1} \in \{-1, +1\}$ determines a sign of the reference curvature radius $R_{[i-1]\mathrm{r}}$ for the $(i-1)$st vehicle's segment. Only the selection (37) guarantees satisfaction of the anti-jackknife condition C4. Note, however, that by changing the bi-valued factor ξ_{i-1} for particular segments one can compute all possible solutions of (31), also those not satisfying C4 (cf. Fig. 4 for $N = 3$). Upon (32) and the forms of (33)–(36), it is not difficult to check that there exist (at least) 2^N distinct solutions to (31) corresponding to the same guidance-reference with a constant motion curvature.

4.3. Reconstruction for the varying-curvature guidance-references

If the guidance-reference is curvature-varying (denoted by $\omega_{N\mathrm{r}}(p)/v_{N\mathrm{r}}(p) = \text{var}$ in Fig. 4), then the joint-reference $\boldsymbol{\beta}_{\mathrm{r}}(p)$ is also varying (with respect to the parametrizing variable p). It is generally impossible to find a closed-form solution of (31) in this case. In particular, for a periodic reference guiding velocity $\boldsymbol{u}_{N\mathrm{r}}(p)$, the joint-reference can be a limit cycle of dynamics (31), see, e.g., [21,41,42]. By analogy to the existence of multiple solutions to (31) for the guidance-references of a constant curvature (see Section 4.2), we conjecture that there exist probably (at least) 2^N different solutions to dynamics (31) corresponding to the same velocity profile $\boldsymbol{u}_{N\mathrm{r}}(p)$. Since we are searching only for the admissible joint-reference $\boldsymbol{\beta}_{\mathrm{r}}(p)$, which satisfies the anti-jackknife condition C4, finding this particular solution is a non-trivial task. The ways of finding the admissible joint-reference depend on the values of the hitching offsets present in a vehicle chain.

4.3.1. The case of sign-homogeneous off-axle hitching

In a special case, if all the hitching offsets in the N-trailer vehicle are non-zero and have the same sign (the nSNT vehicle with sign-homogeneous hitching: all $L_{\mathrm{h}i}$ are positive or all are negative), finding an admissible solution to Problem 1 is (asymptotically) possible by numerically integrating Eq. (31) for an appropriately selected initial condition – see the alternative case B denoted by a dashed line in Fig. 4. However, this approach has some fundamental limitations. To be more strict, let us denote by $\hat{\boldsymbol{\beta}}_{\mathrm{r}}(p)$ a numerical solution of Eq. (31) for $\boldsymbol{P}_j \overset{(28)}{=} \boldsymbol{J}_j^{-1}$, that is, when $\hat{\boldsymbol{\beta}}_{\mathrm{r}}(p)$ satisfies the following equation

$$\hat{\boldsymbol{\beta}}_{\mathrm{r}}'(p) = \boldsymbol{S}_{\beta}(\hat{\boldsymbol{\beta}}_{\mathrm{r}}(p)) \prod_{j=1}^{N} \boldsymbol{J}_j^{-1}(\hat{\boldsymbol{\beta}}_{j\mathrm{r}}(p)) \boldsymbol{u}_{N\mathrm{r}}(p), \tag{38}$$

for some initial condition $\hat{\boldsymbol{\beta}}_{\mathrm{r}}^{\mathrm{init}}$. Recalling the results of [27], concerning a stability analysis of the joint-angle dynamics (see also the study of nonminimum-phasiness for the N-trailers in [15]), and upon simulation investigations, one shall expect that the solution $\hat{\boldsymbol{\beta}}_{\mathrm{r}}(p)$ of Eq. (38) will asymptotically converge to the sought admissible joint-reference $\boldsymbol{\beta}_{\mathrm{r}}(p)$, at least locally for $\|\hat{\boldsymbol{\beta}}_{\mathrm{r}}^{\mathrm{init}} - \boldsymbol{\beta}_{\mathrm{r}}^{\mathrm{init}}\|$ small enough[2], if one of the conditions is met:

- I1: the integration of (38) is performed along a forward p-flow ($\mathrm{d}p > 0$) and $\forall\, i \in \mathcal{I}_{\mathrm{off}}\ (v_{N\mathrm{r}}(p)/L_{\mathrm{h}i}) < 0$,
- I2: the integration of (38) is performed along a backward p-flow ($\mathrm{d}p < 0$) and $\forall\, i \in \mathcal{I}_{\mathrm{off}}\ (v_{N\mathrm{r}}(p)/L_{\mathrm{h}i}) > 0$.

Remark 6. For any of the conditions, I1 or I2, a terminal accuracy of the solution $\hat{\boldsymbol{\beta}}_{\mathrm{r}}(p)$, represented by the norm $\|\hat{\boldsymbol{\beta}}_{\mathrm{r}}(p) - \boldsymbol{\beta}_{\mathrm{r}}(p)\|$, depends on an integration horizon. It means that an arbitrarily good accuracy can be obtained by integration of (38) along a sufficiently long horizon of the parametrizing variable p.

Both inequalities formulated in I1 and I2 require the common signs of all the hitching offsets. Thus, in the case of mixed signs of hitching offsets present in a vehicle chain (that is, when $\exists\, i, j:\ L_{\mathrm{h}i}L_{\mathrm{h}j} < 0$), a numerical integration of (38), either along a forward p-flow or along a backward p-flow, is no longer helpful in finding an admissible joint-reference, because the integral of (38) is not convergent to a solution satisfying C4. In this case, it usually converges to the other solution satisfying (27), but violating C4.

4.3.2. The case where conditions I1 and I2 are violated

If both the conditions from the previous subsection, I1 and I2, are not satisfied, or if the numerical integration of Eq. (31) is not a preferred approach to find a solution to Problem 1, one may formulate an alternative method which allows finding an admissible joint-reference $\boldsymbol{\beta}_{\mathrm{r}}(p)$ for the nSNT and GNT kinematics with any type of hitching. We propose to formulate such a method in a form of some optimization task, denoted as case C in Fig. 4, which resembles a curve fitting problem, [31]. The method is valid under assumption that a prescribed reference guiding velocity $\boldsymbol{u}_{N\mathrm{r}}(p)$ is periodic, i.e.,

$$\forall\, p \quad \boldsymbol{u}_{N\mathrm{r}}(p) = \boldsymbol{u}_{N\mathrm{r}}(p+P), \tag{39}$$

where $0 < P < \infty$ denotes a period in a domain of the parametrizing variable p. The assumption on the periodicity of $\boldsymbol{u}_{N\mathrm{r}}(p)$, although limiting to some extent, can still be useful in numerous practical applications. Namely, the periodicity of $\boldsymbol{u}_{N\mathrm{r}}(p)$ may naturally correspond to a closed (periodic) guidance-reference when $\boldsymbol{q}_{N\mathrm{r}}(p+P) = \boldsymbol{q}_{N\mathrm{r}}(p)$, which in turn corresponds to a closed-curve image on a motion plane. In this case, the admissible joint-reference $\boldsymbol{\beta}_{\mathrm{r}}(p)$ should be also periodic, being a limit cycle of dynamics (31). However, there exists another possibility – one can design the non-periodic guidance-references (e.g., by using splines) which correspond to the open-curve images on a motion plane, but impose the same values of the reference guiding-velocity on their ends, that is, when $\boldsymbol{q}_{N\mathrm{r}}(p+P) \neq \boldsymbol{q}_{N\mathrm{r}}(p)$ but $\boldsymbol{u}_{N\mathrm{r}}(p+P) = \boldsymbol{u}_{N\mathrm{r}}(p)$. Examples of both mentioned types of the guidance-references with a periodic reference guiding velocities are illustrated in Fig. 5.

Remark 7. The method explained below can be used for all the guidance-references $\boldsymbol{q}_{N\mathrm{r}}$ having images in the forms either of the closed curves homotopic to a circle or open curves homotopic to a straight line segment on a plane.

[2] One usually observes a large basin of attraction for $\hat{\boldsymbol{\beta}}_{\mathrm{r}}(p)$, admitting a relatively large difference $\|\hat{\boldsymbol{\beta}}_{\mathrm{r}}^{\mathrm{init}} - \boldsymbol{\beta}_{\mathrm{r}}^{\mathrm{init}}\|$; it makes a selection of the initial condition $\hat{\boldsymbol{\beta}}_{\mathrm{r}}^{\mathrm{init}}$ relatively easy (often taken as zero).

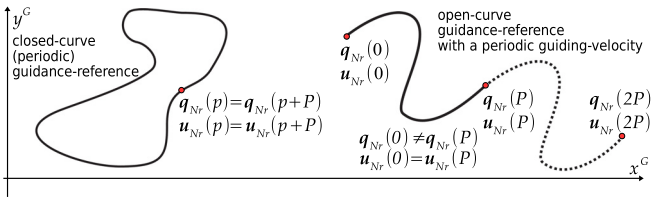

Fig. 5. Illustration of the guidance-references $\boldsymbol{q}_{N\mathrm{r}}(p)$ characterized by the closed-curve (left) and open-curve (right) images on a motion plane, both having a periodic reference guiding velocity $\boldsymbol{u}_{N\mathrm{r}}(p)$.

We will explain a proposed computational method for this case by rewriting (31) in a shorter form

$$\boldsymbol{\beta}_{\mathrm{r}}'(p) = \boldsymbol{f}\big(\boldsymbol{\beta}_{\mathrm{r}}(p), \boldsymbol{u}_{N\mathrm{r}}(p)\big) = \boldsymbol{f}\big(\boldsymbol{\beta}_{\mathrm{r}}(p), p\big), \tag{40}$$

where $\boldsymbol{f} = [f_1(\boldsymbol{\beta}_{\mathrm{r}}(p), p)\ \ldots\ f_N(\boldsymbol{\beta}_{\mathrm{r}}(p), p)]^\top$, and the prescribed velocity $\boldsymbol{u}_{N\mathrm{r}}(p)$ satisfies assumption (39).

Due to the presence of constraint (29), and to better explain the computational scheme, let us partition the vector of joint angles $\boldsymbol{\beta}$ into two subvectors:

$$\boldsymbol{\beta}_{\mathrm{off}} \triangleq [\ldots \beta_j \ldots]^\top \quad \text{for } j \in \mathcal{I}_{\mathrm{off}},$$
$$\boldsymbol{\beta}_{\mathrm{on}} \triangleq [\ldots \beta_s \ldots]^\top \quad \text{for } s \in \mathcal{I}_{\mathrm{on}},$$

such that $\dim(\boldsymbol{\beta}_{\mathrm{off}}) + \dim(\boldsymbol{\beta}_{\mathrm{on}}) = \dim(\boldsymbol{\beta}) = N$. By analogy, let us partition the joint-reference $\boldsymbol{\beta}_r$ by introducing

$$\boldsymbol{\beta}_{\mathrm{r}\mathrm{off}} \triangleq [\ldots \beta_{j\mathrm{r}} \ldots]^\top \quad \text{for } j \in \mathcal{I}_{\mathrm{off}},$$
$$\boldsymbol{\beta}_{\mathrm{r}\mathrm{on}} \triangleq [\ldots \beta_{s\mathrm{r}} \ldots]^\top \quad \text{for } s \in \mathcal{I}_{\mathrm{on}},$$

such that $\dim(\boldsymbol{\beta}_{\mathrm{r}\mathrm{off}}) + \dim(\boldsymbol{\beta}_{\mathrm{r}\mathrm{on}}) = \dim(\boldsymbol{\beta}_{\mathrm{r}}) = N$. The joint-reference kinematics (40) can be now partitioned as follows

$$\boldsymbol{\beta}_{\mathrm{r}\mathrm{off}}'(p) = \boldsymbol{f}_{\mathrm{off}}\big(\boldsymbol{\beta}_{\mathrm{r}\mathrm{off}}(p), \boldsymbol{\beta}_{\mathrm{r}\mathrm{on}}(p), p\big), \tag{41}$$

$$\boldsymbol{\beta}_{\mathrm{r}\mathrm{on}}'(p) = \boldsymbol{f}_{\mathrm{on}}\big(\boldsymbol{\beta}_{\mathrm{r}\mathrm{off}}(p), \boldsymbol{\beta}_{\mathrm{r}\mathrm{on}}(p), p\big), \tag{42}$$

where

$$\boldsymbol{f}_{\mathrm{off}} \triangleq [\ldots f_j\big(\boldsymbol{\beta}_{\mathrm{r}\mathrm{off}}(p), \boldsymbol{\beta}_{\mathrm{r}\mathrm{on}}(p), p\big) \ldots]^\top \quad \text{for } j \in \mathcal{I}_{\mathrm{off}},$$
$$\boldsymbol{f}_{\mathrm{on}} \triangleq [\ldots f_s\big(\boldsymbol{\beta}_{\mathrm{r}\mathrm{off}}(p), \boldsymbol{\beta}_{\mathrm{r}\mathrm{on}}(p), p\big) \ldots]^\top \quad \text{for } s \in \mathcal{I}_{\mathrm{on}},$$

such that $\dim(\boldsymbol{f}_{\mathrm{off}}) + \dim(\boldsymbol{f}_{\mathrm{on}}) = \dim(\boldsymbol{f}) = N$.

Since the kinematics (42) must preserve constraint (29), the angles $\boldsymbol{\beta}_{\mathrm{r}\mathrm{on}}$ will be computed directly upon (29). Thus, only angles $\boldsymbol{\beta}_{\mathrm{r}\mathrm{off}}$ will be searched numerically as non-constrained ones. Let us denote by $\hat{\boldsymbol{\beta}}_{\mathrm{r}} = [\hat{\beta}_{1\mathrm{r}}\ \ldots\ \hat{\beta}_{N\mathrm{r}}]^\top$ an approximation of the sought solution to (40), composed of $\hat{\boldsymbol{\beta}}_{\mathrm{r}\mathrm{off}}(p) = [\ldots \hat{\beta}_{j\mathrm{r}} \ldots]^\top$, $j \in \mathcal{I}_{\mathrm{off}}$ and $\hat{\boldsymbol{\beta}}_{\mathrm{r}\mathrm{on}}(p) = [\ldots \hat{\beta}_{s\mathrm{r}} \ldots]^\top$, $s \in \mathcal{I}_{\mathrm{on}}$, such that $\dim(\hat{\boldsymbol{\beta}}_{\mathrm{r}\mathrm{off}}) + \dim(\hat{\boldsymbol{\beta}}_{\mathrm{r}\mathrm{on}}) = \dim(\hat{\boldsymbol{\beta}}_{\mathrm{r}}) = N$. We express the components of $\hat{\boldsymbol{\beta}}_{\mathrm{r}\mathrm{off}}(p)$ in a parametrized form

$$\hat{\beta}_{j\mathrm{r}}(p) = \boldsymbol{\Phi}^\top(p)\boldsymbol{w}_j, \qquad j \in \mathcal{I}_{\mathrm{off}}, \tag{43}$$

where $\boldsymbol{\Phi}(p) \in \mathbb{R}^w$ is a vector of Fourier-basis functions, whereas $\boldsymbol{w}_j = [w_{1j}\ \ldots\ w_{wj}]^\top \in \mathbb{R}^w$ is a vector of parameters for the jth component of the reference $\hat{\boldsymbol{\beta}}_{\mathrm{r}\mathrm{off}}(p)$. We define an approximation error

$$\boldsymbol{\epsilon}(p, \boldsymbol{w}) \triangleq \hat{\boldsymbol{\beta}}_{\mathrm{r}\mathrm{off}}'(p) - \boldsymbol{f}_{\mathrm{off}}(\hat{\boldsymbol{\beta}}_{\mathrm{r}\mathrm{off}}(p), \boldsymbol{\beta}_{\mathrm{r}\mathrm{on}}^*(p), p) \tag{44}$$
$$\overset{(43)}{=} \begin{bmatrix} \vdots \\ \boldsymbol{\Phi}'^\top(p)\boldsymbol{w}_j \\ \vdots \end{bmatrix} - \boldsymbol{f}\left(\begin{bmatrix} \vdots \\ \boldsymbol{\Phi}^\top(p)\boldsymbol{w}_j \\ \vdots \end{bmatrix}, \boldsymbol{\beta}_{\mathrm{r}\mathrm{on}}^*(p), p\right),$$

where $\boldsymbol{w} = [\dots \boldsymbol{w}_j^\top \dots]^\top \in \mathbb{R}^{w|\mathcal{I}_{\text{off}}|}$, $j \in \mathcal{I}_{\text{off}}$, while $\boldsymbol{\Phi}'(p) = \mathrm{d}\boldsymbol{\Phi}(p)/\mathrm{d}p$ can be derived analytically. Note that (44) is a difference between the left- and the right-hand side of (41), evaluated along the approximating joint-reference $\hat{\boldsymbol{\beta}}_{\mathrm{r}}$ composed of $\hat{\boldsymbol{\beta}}_{\mathrm{r}\text{off}}$ and $\hat{\boldsymbol{\beta}}_{\mathrm{r}\text{on}} := \boldsymbol{\beta}^*_{\mathrm{r}\text{on}}$, where $\boldsymbol{\beta}^*_{\mathrm{r}\text{on}} \triangleq [\dots \beta^*_{s\mathrm{r}} \dots]^\top$ and

$$\beta^*_{s\mathrm{r}} \overset{(29)}{=} \operatorname{Atan2}(\zeta_{\mathrm{r}} L_s \omega_{s\mathrm{r}}, \zeta_{\mathrm{r}} v_{s\mathrm{r}}), \quad s \in \mathcal{I}_{\text{on}}. \tag{45}$$

Computation of (45) is always possible thanks to the inverse velocity kinematics (see Section 2.3), where the components of velocity

$$\boldsymbol{u}_{s\mathrm{r}} = \begin{bmatrix} \omega_{s\mathrm{r}} \\ v_{s\mathrm{r}} \end{bmatrix} \overset{(26)}{=} \prod_{j=s+1}^{N} \boldsymbol{P}_j(\hat{\beta}_{j\mathrm{r}}, \boldsymbol{u}_{j\mathrm{r}}, \boldsymbol{u}'_{j\mathrm{r}}) \boldsymbol{u}_{N\mathrm{r}} \tag{46}$$

can be computed upon the available angles $\hat{\beta}_{[s+1]\mathrm{r}}, \dots, \hat{\beta}_{N\mathrm{r}}$, and upon the prescribed velocity $\boldsymbol{u}_{N\mathrm{r}}(p)$ and its appropriate derivatives. It is worth emphasizing, that the substitution $\hat{\boldsymbol{\beta}}_{\mathrm{r}\text{on}} := \boldsymbol{\beta}^*_{\mathrm{r}\text{on}}$ is very important for the sake of a convergence of the numerical algorithm proposed in a sequel.

For the purpose of numerical search for $\hat{\boldsymbol{\beta}}_{\mathrm{r}\text{off}}$, the approximation error (44) is sampled in some (evenly distributed) points with a sampling interval $P_s > 0$, being a sufficiently small fraction of period P, leading to samples $\boldsymbol{\epsilon}(kP_s, \boldsymbol{w})$, where $k = 0, 1, \dots, M-1$, and MP_s is an integer multiplicity of P. By collecting the error samples in a vector

$$\boldsymbol{e}(\boldsymbol{w}) = \begin{bmatrix} \boldsymbol{\epsilon}(0, \boldsymbol{w}) \\ \boldsymbol{\epsilon}(P_s, \boldsymbol{w}) \\ \vdots \\ \boldsymbol{\epsilon}((M-1)P_s, \boldsymbol{w}) \end{bmatrix} \in \mathbb{R}^{|\mathcal{I}_{\text{off}}|M},$$

one can express the problem of finding the approximating reference $\hat{\boldsymbol{\beta}}_{\mathrm{r}\text{off}}(p)$ parametrized by (43) as a *curve fitting* optimization task

$$\hat{\boldsymbol{w}} = \min_{\boldsymbol{w}} K_e(\boldsymbol{w}), \quad K_e(\boldsymbol{w}) \triangleq \boldsymbol{e}^\top(\boldsymbol{w})\, \boldsymbol{e}(\boldsymbol{w}).$$

From now on, one can apply various available numerical optimization tools to solve the above unconstrained least squares problem, [32]. Since it is not of our objective to indicate the most efficient optimization tool for the task, we would like to show that it can be solved with a basic, properly initialized, Newton-like iterative algorithm

$$\hat{\boldsymbol{w}}(l) = \hat{\boldsymbol{w}}(l-1) - \kappa \boldsymbol{\Lambda}^\sharp(\hat{\boldsymbol{w}}(l-1)) \boldsymbol{e}(\hat{\boldsymbol{w}}(l-1)), \tag{47}$$

where $l \in \mathbb{N}$ is an iteration number, $\kappa > 0$ is a design factor, $\sharp$ denotes the left-pseudoinverse operator, and a form of matrix $\boldsymbol{\Lambda}(\boldsymbol{w}) \triangleq \frac{\mathrm{d}\boldsymbol{e}(\boldsymbol{w})}{\mathrm{d}\boldsymbol{w}} \in \mathbb{R}^{|\mathcal{I}_{\text{off}}|M \times w|\mathcal{I}_{\text{off}}|}$ can be either computed analytically, thanks to the form of error (44), or approximated numerically.

Since we conjecture that for $\boldsymbol{u}_{N\mathrm{r}}(p)$ satisfying (39) the Eq. (40) has (at least) 2^N periodic solutions, one has to expect that iteration (47) will be only locally convergent to the admissible solution satisfying condition C4. Therefore, the key issue is to properly initialize (47) by finding a favourable initial condition $\hat{\boldsymbol{w}}(0) := \check{\boldsymbol{w}}$. To this purpose, we propose to initialize iteration (47) with $\check{\boldsymbol{w}} = [\dots \check{\boldsymbol{w}}_j^\top \dots]^\top \in \mathbb{R}^{w|\mathcal{I}_{\text{off}}|}$, where

$$\check{\boldsymbol{w}}_j = \begin{bmatrix} \boldsymbol{\Phi}^\top(0) \\ \vdots \\ \boldsymbol{\Phi}^\top((M-1)P_s) \end{bmatrix}^\sharp \begin{bmatrix} \check{\beta}_{j\mathrm{r}}(0) \\ \vdots \\ \check{\beta}_{j\mathrm{r}}((M-1)P_s) \end{bmatrix}, \quad j \in \mathcal{I}_{\text{off}},$$

are obtained using $\check{\beta}_{j\mathrm{r}}$ computed upon formulas (32)–(37) for a constant-curvature initial *prototype* curve, homotopic to a $\mathbb{R}^2$-image of the considered guidance-reference $\boldsymbol{q}_{N\mathrm{r}}(p)$ (e.g., a circle for the closed-curve images or a straight-line segment for the open-curve images). By gradually deforming the prototype curve (using a homotopy map) in a finite number of $\mu \in \mathbb{N}$ stages, and treating an obtained solution in every stage as an initial condition for the next stage, one can locally guide the iteration process (47) within these μ stages to an admissible (approximate) solution satisfying C4 (see, e.g., [1]).

Summarizing, the reconstructed joint-reference $\hat{\boldsymbol{\beta}}_{\mathrm{r}}(p)$, approximating the sought admissible solution of (40), is composed of the joint-references $\hat{\boldsymbol{\beta}}_{\mathrm{r}\text{off}}(p) = \boldsymbol{\Phi}^\top(p)\hat{\boldsymbol{w}}_j$, with $\hat{\boldsymbol{w}}_j$ found by the numerical algorithm (47), and of the references $\hat{\boldsymbol{\beta}}_{\mathrm{r}\text{on}}(p) = \boldsymbol{\beta}^*_{\mathrm{r}\text{on}}(p)$ computed upon (45)-(46).

Remark 8. An accuracy of the approximation $\hat{\boldsymbol{\beta}}_{\mathrm{r}\text{off}}(p)$ depends on a number of basis functions used in a construction of $\boldsymbol{\Phi}(p)$, and on a precision with which the parameters $\hat{\boldsymbol{w}}$ are found by the iterative process (47). Hence, by increasing a number of Fourier-basis functions (see Section 5), and by sampling the error (44) dense enough, one can obtain the approximation $\hat{\boldsymbol{\beta}}_{\mathrm{r}}(p)$ of a sought reference $\boldsymbol{\beta}_{\mathrm{r}}(p)$ with an accuracy level required by a particular application.

Remark 9. For the differentially flat SNT kinematics, the reconstruction problem reduces to the computations of $\boldsymbol{\beta}_{\mathrm{r}}(p) \equiv \boldsymbol{\beta}^*_{\mathrm{r}\text{on}}(p)$ according to formulas (45) and (46).

The proposed reconstruction method leads to a *prototype* reference $\boldsymbol{q}_{\mathrm{r}}(p)$ which can be treated as a parametrized path, or can be used to compute a corresponding reference trajectory $\boldsymbol{q}_{\mathrm{r}}(t)$. In the latter case, one needs to select a mapping $p \mapsto t$ coming from the differential relationship $\mathrm{d}p = f_p(t)\mathrm{d}t$, where $f_p(t)$ can be an imposed (linear or non-linear) function expressing how the parameter p scales into time. As a consequence, the reference guiding velocity $\tilde{\boldsymbol{u}}_{N\mathrm{r}}(t) = \boldsymbol{u}_{N\mathrm{r}}(p) f_p(t)$.

Remark 10. One could alternatively address the inversion problem for the N-trailers by solving an appropriately defined constrained continuous-time optimal control problem (CCTOCP), where the prescribed output-reference (24) forms an additional equality constraint, or where a deviation between (24) and (5) is minimized (see, e.g., [5,6,14,25,26,40] and references therein for exemplary applications of the CCTOCP to motion planning for nonholonomic systems, including N-trailers). The direct methods with collocation, being commonly employed to find a solution of CCTOCP [20,38], reformulate the continuous-time optimal control problem into a finite dimensional nonlinear programming problem (NLP), [12]. Although such an approach is quite general, and elegant to some extent, its practical efficiency (despite the existence of specialized computational tools like ACADO [17] and others [32]) may be limited for the complex N-trailer kinematics under constraints, especially when a number of trailers is large. The authors of [5,25] report some practical difficulties when employing the NLP to constrained nonholonomic systems and N-trailers, stressing an importance of an appropriate selection of a favorable initial condition for iterative computations, and propose to support a numerical optimization process with a continuation method. The solution proposed in the current section corresponds, in some sense, to the observations reported in [5,25], by reducing the inversion problem (thanks to postulated periodicity (39)) to the *unconstrained* least squares *curve fitting* task. This classical, well known and relatively simple, numerical task can be successfully computed even with a basic Newton-like algorithm when started from the suggested initial condition $\check{\boldsymbol{w}}$ and supported by a continuation method. In contrast to the NLP, the proposed method does not require any discretization of the control signals nor the equations of system dynamics, avoiding a possible negative influence of the resultant discretization errors on a solution accuracy.

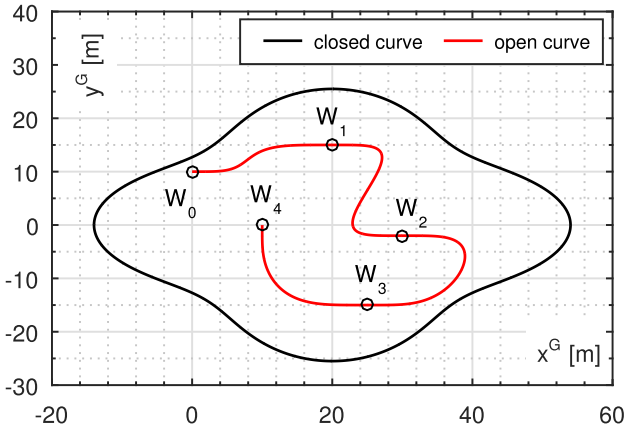

Fig. 6. Images (plane curves) of the two guidance-references selected for the 3-trailer vehicles used in the numerical examples: the CLOSED-curve reference (the black Lissajous curve) and the OPEN-curve reference (the 9th-degree spline highlighted in red).

The inherently restricted flexibility of the inversion problem (due to fixing the output-reference) implies some fundamental limitations of the proposed solution. Namely, since the N-trailers with off-axle hitching can exhibit in particular motion conditions the unavoidable nonminimum-phase effects (like an initial undershoot or initial oscillations) in a response of the angular configuration variables, [15], it seems generally impossible to find the admissible joint-references satisfying C4 for *any arbitrarily prescribed* guidance-reference (even those admissible for the unicycle kinematics). Therefore, in some cases one should conclude that for the prescribed output-reference the inversion problem does not have an admissible solution for a particular N-trailer. Furthermore, as a consequence of postulate (39), the method is searching for an admissible *limit cycle* in the space of joint angles. Hence, it does not allow imposing *arbitrary* boundary values $\boldsymbol{\beta}_{\mathrm{r}}(0)$ and $\boldsymbol{\beta}_{\mathrm{r}}(P)$ at the beginning and at the end of a predefined guidance-reference. To force some particular values for $\boldsymbol{\beta}_{\mathrm{r}}(0)$ and $\boldsymbol{\beta}_{\mathrm{r}}(P)$ one could, for instance, appropriately deform the guidance-reference (similarly to the approach proposed in [16]) which is, however, a non-trivial task and shifts the original inversion problem closer to the motion planning, not addressed in this paper.

5. Numerical examples

We present four examples of reconstructing the joint-references for 3-trailer vehicles ($N=3$), using the iterative algorithm (47) with $\kappa=1$, in the case of a forward reference motion ($\mathrm{sgn}(v_{N\mathrm{r}}(p))=+1$) and backward reference motion ($\mathrm{sgn}(v_{N\mathrm{r}}(p))=-1$) imposed along two types of guidance-references. The selected guidance-references correspond to the following images on a motion plane (see Fig. 6): the Lissajous CLOSED-curve reference

$$x_{3\mathrm{r}}(p) \triangleq A_{\mathrm{r}}(p)\sin(2\pi\, p)+20.0,$$
$$y_{3\mathrm{r}}(p) \triangleq 0.75A_{\mathrm{r}}(p)\sin(2\pi\, p+\pi/2),$$
$$\theta_{3\mathrm{r}}(p)=\mathrm{Atan2}\big(\zeta_r\, y'_{3\mathrm{r}}(p),\zeta_r\, x'_{3\mathrm{r}}(p)\big),$$

computed with $A_{\mathrm{r}}(p)=4.0\cos(8\pi\, p)+30.0$, and the OPEN-curve reference using the 9th-degree spline composed of four polynomial segments

$$x_{3\mathrm{r}}(p) \triangleq \eta_9 p^{(9)}+\ldots+\eta_1 p^{(1)}+\eta_0,$$
$$y_{3\mathrm{r}}(p) \triangleq \nu_9 p^{(9)}+\ldots+\nu_1 p^{(1)}+\nu_0,$$
$$\theta_{3\mathrm{r}}(p)=\mathrm{Atan2}\big(\zeta_r\, y'_{3\mathrm{r}}(p),\zeta_r\, x'_{3\mathrm{r}}(p)\big),$$

going through five net-points $W_j(p_j)=(\Theta_j,X_j,Y_j)$, in ([rad],[m],[m]), $j=0,\ldots,4$, where $W_0(p_0)=(0,0,10)$, $W_1(p_1)=(0,20,15)$, $W_2(p_2)=(0,30,-2)$, $W_3(p_3)=(\pi,25,-15)$, $W_4(p_4)=(\pi/2,10,0)$, with corresponding reference longitudinal velocities (in units[3] [j]): $v_{3\mathrm{r}}(p_0)=80$, $v_{3\mathrm{r}}(p_1)=120$, $v_{3\mathrm{r}}(p_2)=120$, $v_{3\mathrm{r}}(p_3)=120$, $v_{3\mathrm{r}}(p_4)=80$.

The polynomials were concatenated in a way to ensure a zero acceleration, a zero jerk, and a zero snap at all the net-points. A sufficiently high continuity degree of the defined polynomials allowed reducing the well known Gibbs effect when approximating a non-smooth curve by a finite Fourier basis, see [7]. Both the guidance-references have been parametrized with a normalized parameter $p\in[0,1]$. The joint-references were computed in both cases of the guidance-references for the following two types of 3-trailer kinematics (cf. Fig. 2): the non-Standard 3-Trailer (nS3T) and the Generalized 3-Trailer (G3T) with kinematic parameters collected in Table 1.

The selected 3-trailers represent kinematics of two popular Large Capacity Vehicles used in a freight transportation today. The nS3T structure consists of a semitrailer (put on a tractor) and two one-axle trailers attached in a chain. The G3T structure comprises a semitrailer (put on a tractor) and an attached dolly with an additional semitrailer put on the dolly.

In the case of nS3T vehicle, $\boldsymbol{\beta}_{\mathrm{r}}\equiv\boldsymbol{\beta}_{\mathrm{roff}}$, thus $\mathcal{I}_{\mathrm{on}}=\emptyset$. A structure of the exosystem (25) comes from the following inverse velocity kinematics (cf. (26))

$$\boldsymbol{u}_{0\mathrm{r}}^{\mathrm{nS3T}} \overset{(28)}{=} \boldsymbol{J}_1^{-1}(\beta_{1\mathrm{r}})\boldsymbol{J}_2^{-1}(\beta_{2\mathrm{r}})\boldsymbol{J}_3^{-1}(\beta_{3\mathrm{r}})\boldsymbol{u}_{3\mathrm{r}},$$

which corresponds to example E1 addressed in Section 2.4. For the considered G3T vehicle, $\boldsymbol{\beta}_{\mathrm{roff}}=[\beta_{1\mathrm{r}}\ \ \beta_{2\mathrm{r}}]^\top$, $\mathcal{I}_{\mathrm{off}}=\{1,2\}$, and $\boldsymbol{\beta}_{\mathrm{ron}}=[\beta_{3\mathrm{r}}]$, $\mathcal{I}_{\mathrm{on}}=\{3\}$. In this case, the inverse velocity kinematics takes the form (cf. (26))

$$\boldsymbol{u}_{0\mathrm{r}}^{\mathrm{G3T}} \overset{(28)}{=} \boldsymbol{J}_1^{-1}(\beta_{1\mathrm{r}})\boldsymbol{J}_2^{-1}(\beta_{2\mathrm{r}})\boldsymbol{H}_3(\beta_{3\mathrm{r}}^*,\boldsymbol{u}_{3\mathrm{r}},\boldsymbol{u}'_{3\mathrm{r}})\boldsymbol{u}_{3\mathrm{r}},$$

corresponding to example E2 from Section 2.4, where

$$\beta_{3\mathrm{r}}^* \overset{(29)}{=} \mathrm{Atan2}(\zeta_{\mathrm{r}}L_3\omega_{3\mathrm{r}},\zeta_{\mathrm{r}}v_{3\mathrm{r}}),$$

and

$$\boldsymbol{u}_{3\mathrm{r}}=\begin{bmatrix}\omega_{3\mathrm{r}}\\ v_{3\mathrm{r}}\end{bmatrix}=\begin{bmatrix}(y''_{3\mathrm{r}}x'_{3\mathrm{r}}-y'_{3\mathrm{r}}x''_{3\mathrm{r}})/(x'^2_{3\mathrm{r}}+y'^2_{3\mathrm{r}})\\ \zeta_{\mathrm{r}}\sqrt{x'^2_{3\mathrm{r}}+y'^2_{3\mathrm{r}}}\end{bmatrix},$$

(under condition C4, $\zeta_{\mathrm{r}}:=+1$ for the forward reference motion, and $\zeta_{\mathrm{r}}:=-1$ for the backward reference motion), while $\boldsymbol{u}'_{3\mathrm{r}}=[\omega'_{3\mathrm{r}}\ \ v'_{3\mathrm{r}}]^\top$ is a derivative of the above formula with respect to p. For both the nS3T and G3T vehicles, the kinematic matrix $\boldsymbol{S}(\boldsymbol{q}_{\mathrm{r}}(p))$ reduces to the form (cf. (4))

$$\boldsymbol{S}(\boldsymbol{q}_{\mathrm{r}}(p))=\begin{bmatrix}\boldsymbol{c}^\top\boldsymbol{\Gamma}_1(\beta_{1\mathrm{r}})\\ \boldsymbol{c}^\top\boldsymbol{\Gamma}_2(\beta_{2\mathrm{r}})\boldsymbol{J}_1(\beta_{1\mathrm{r}})\\ \boldsymbol{c}^\top\boldsymbol{\Gamma}_3(\beta_{3\mathrm{r}})\boldsymbol{J}_2(\beta_{2\mathrm{r}})\boldsymbol{J}_1(\beta_{1\mathrm{r}})\\ \hline \boldsymbol{c}^\top\boldsymbol{J}_3(\beta_{3\mathrm{r}})\boldsymbol{J}_2(\beta_{2\mathrm{r}})\boldsymbol{J}_1(\beta_{1\mathrm{r}})\\ \boldsymbol{d}^\top\boldsymbol{J}_3(\beta_{3\mathrm{r}})\boldsymbol{J}_2(\beta_{2\mathrm{r}})\boldsymbol{J}_1(\beta_{1\mathrm{r}})\mathrm{c}\theta_{3\mathrm{r}}\\ \boldsymbol{d}^\top\boldsymbol{J}_3(\beta_{3\mathrm{r}})\boldsymbol{J}_2(\beta_{2\mathrm{r}})\boldsymbol{J}_1(\beta_{1\mathrm{r}})\mathrm{s}\theta_{3\mathrm{r}}\end{bmatrix}=\begin{bmatrix}\boldsymbol{S}_\beta(\boldsymbol{\beta}_{\mathrm{r}})\\ \hline \boldsymbol{S}_3(\boldsymbol{\beta}_{\mathrm{r}},\boldsymbol{q}_{3\mathrm{r}})\end{bmatrix},$$

where $\boldsymbol{\beta}_{\mathrm{r}}=[\beta_{1\mathrm{r}}\ \beta_{2\mathrm{r}}\ \beta_{3\mathrm{r}}]^\top$ and $\boldsymbol{q}_{3\mathrm{r}}=[\theta_{3\mathrm{r}}\ x_{3\mathrm{r}}\ y_{3\mathrm{r}}]^\top$. One observes that the function $\boldsymbol{f}(\boldsymbol{\beta}_{\mathrm{r}}(p),p)$, introduced in (40), takes in this case the form: $\boldsymbol{f}(\boldsymbol{\beta}_{\mathrm{r}}(p),p)=\boldsymbol{S}_\beta(\boldsymbol{\beta}_{\mathrm{r}})\boldsymbol{u}_{0\mathrm{r}}$, where $\boldsymbol{u}_{0\mathrm{r}}:=\boldsymbol{u}_{0\mathrm{r}}^{\mathrm{nS3T}}$ for the nS3T vehicle, and $\boldsymbol{u}_{0\mathrm{r}}:=\boldsymbol{u}_{0\mathrm{r}}^{\mathrm{G3T}}$ for the G3T vehicle.

Results of the exemplary reconstructions, conducted for a number of $n_{\mathrm{h}}=2000$ harmonics, sampled with a sampling interval $P_s=2\cdot10^{-4}$, are presented in Figs. 7 and 8 for kinematics nS3T, and in Figs. 9 and 10 for kinematics G3T.

[3] If p is interpreted in [m], as a curvilinear path length, then $v_{i\mathrm{r}}(p)$ is unitless, while if p is interpreted as time in [s] then $v_{i\mathrm{r}}(p)$ is expressed in [m/s].

Table 1
Values of kinematic parameters selected for the articulated vehicles used in the numerical examples.

Vehicle kinematics	Hitching scheme	Lengths of trailers [m]	Hitching offsets [m]
nS3T	OFF-OFF-OFF	$L_1 = 7.4,\ L_2 = 5.0,\ L_3 = 5.0$	$L_{\mathrm{h}1} = -0.475,\ L_{\mathrm{h}2} = 1.5,\ L_{\mathrm{h}3} = 1.5$
G3T	OFF-OFF-ON	$L_1 = 7.7,\ L_2 = 1.9,\ L_3 = 9.0$	$L_{\mathrm{h}1} = -0.475,\ L_{\mathrm{h}2} = 1.8,\ L_{\mathrm{h}3} = 0.0$

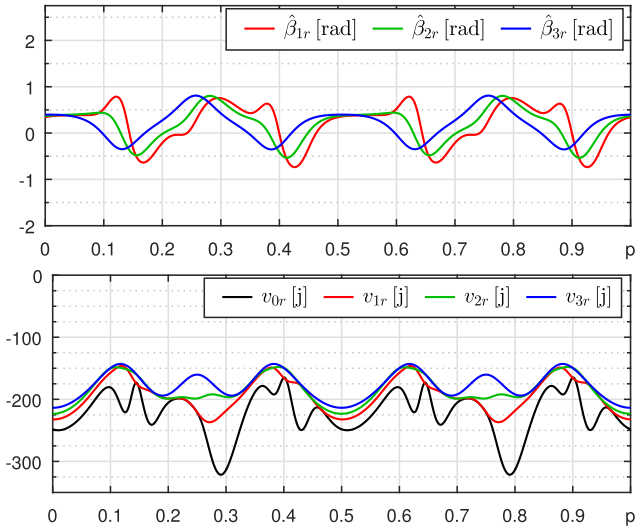

Fig. 7. Evolution of the reconstructed joint-references and the reference longitudinal velocities (backward motion), with respect to a normalized parameter $p \in [0, 1]$, computed for the nS3T kinematics in the case of the CLOSED-curve guidance-reference $\boldsymbol{q}_{3\Gamma}(p)$.

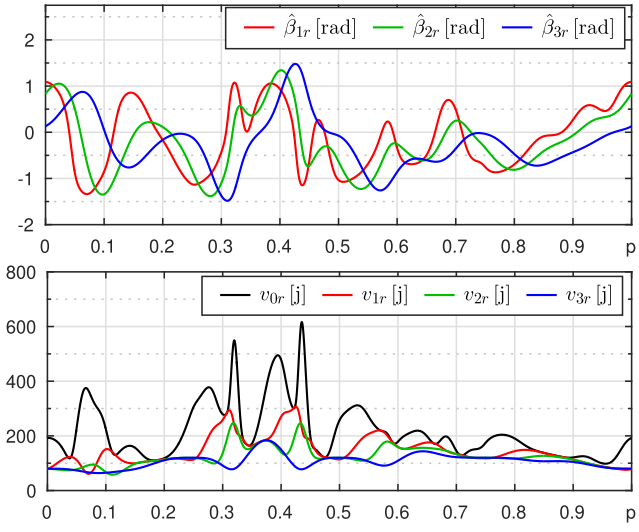

Fig. 8. Evolution of the reconstructed joint-references and the reference longitudinal velocities (forward motion), with respect to a normalized parameter $p \in [0, 1]$, computed for the nS3T kinematics in the case of the OPEN-curve guidance-reference $\boldsymbol{q}_{3\Gamma}(p)$.

An accuracy of the reconstructed joint-references with respect to a number of harmonics n_{h}, used in a Fourier basis in (43), has been assessed upon three quality-criteria:

$$K_1 \triangleq P_s\, \boldsymbol{e}^{\top}(\hat{\boldsymbol{w}})\, \boldsymbol{e}(\hat{\boldsymbol{w}}),$$

$$K_2 \triangleq \int_0^1 \left\| \boldsymbol{q}_{3\Gamma}(\xi) - \hat{\boldsymbol{q}}_{3\Gamma}(\xi) \right\| \mathrm{d}\xi,$$

$$K_3 \triangleq \max_{p\in[0,1]} \left\| \boldsymbol{q}_{3\Gamma}(p) - \hat{\boldsymbol{q}}_{3\Gamma}(p) \right\|_{\infty},$$

where $\hat{\boldsymbol{q}}_{3\Gamma}(p) = \left[\boldsymbol{0}_{3\times 3}\ \boldsymbol{I}_{3\times 3}\right]\check{\boldsymbol{q}}_{\Gamma}(p)$ is an estimated guidance-reference computed upon the reconstructed joint-reference $\hat{\boldsymbol{\beta}}_{\Gamma}(p)$,

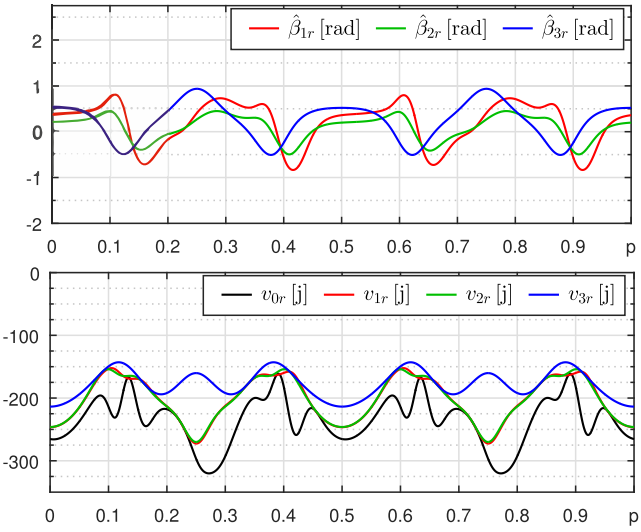

Fig. 9. Evolution of the reconstructed joint-references and the reference longitudinal velocities (backward motion), with respect to a normalized parameter $p \in [0, 1]$, computed for the G3T kinematics in the case of the CLOSED-curve guidance-reference $\boldsymbol{q}_{3\Gamma}(p)$.

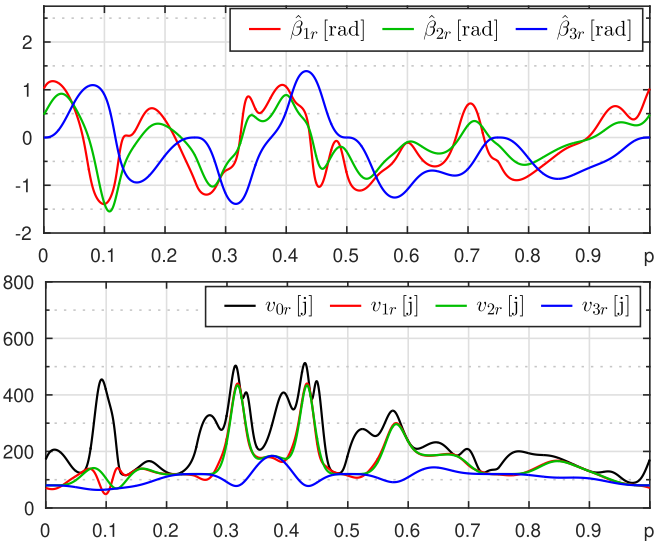

Fig. 10. Evolution of the reconstructed joint-references and the reference longitudinal velocities (forward motion), with respect to a normalized parameter $p \in [0, 1]$, computed for the G3T kinematics in the case of the OPEN-curve guidance-reference $\boldsymbol{q}_{3\Gamma}(p)$.

with $\check{\boldsymbol{q}}_{\Gamma}(p)$ being a solution, for $p \in [0, 1]$, of the differential equation

$$\check{\boldsymbol{q}}'_{\Gamma}(p) = \boldsymbol{S}(\check{\boldsymbol{q}}_{\Gamma}(p)) \prod_{j=1}^{3} \boldsymbol{P}_j(\hat{\beta}_{j\Gamma}(p), \boldsymbol{u}_{j\Gamma}(p), \boldsymbol{u}'_{j\Gamma}(p))\boldsymbol{u}_{3\Gamma}(p), \tag{48}$$

computed for the initial condition $\check{\boldsymbol{q}}_{\Gamma}^{\mathrm{init}} := [\hat{\boldsymbol{\beta}}_{\Gamma}(0)\ \boldsymbol{q}_{3\Gamma}(0)]^{\top}$ taken for the forward reference motion, and $\check{\boldsymbol{q}}_{\Gamma}^{\mathrm{init}} := [\hat{\boldsymbol{\beta}}_{\Gamma}(1)\ \boldsymbol{q}_{3\Gamma}(1)]^{\top}$ taken for the backward reference motion along a prescribed

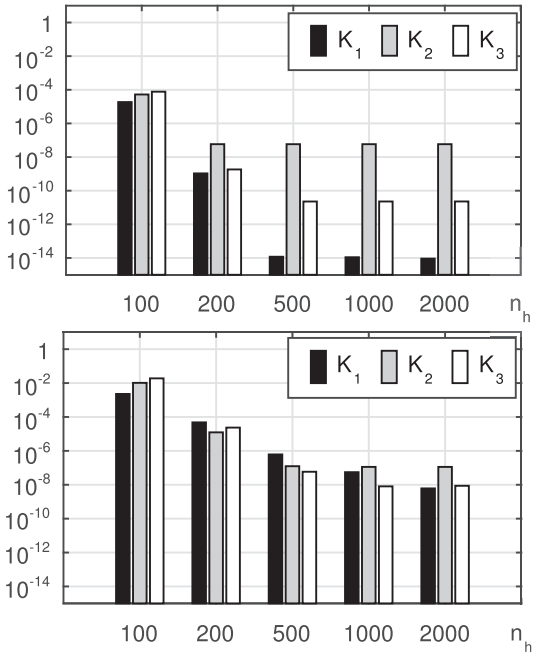

Fig. 11. Values of indexes K_1, K_2, K_3, with respect to a number n_{h} of harmonics used in the Fourier basis, obtained for the nS3T kinematics in the case of the CLOSED-curve (upper plot) and the OPEN-curve (lower plot) guidance-reference $\boldsymbol{q}_{3\mathrm{r}}(p)$.

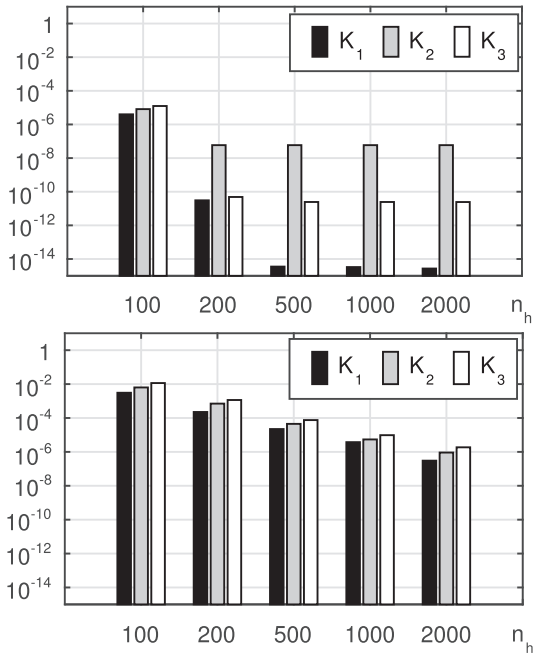

Fig. 12. Values of indexes K_1, K_2, K_3, with respect to a number n_{h} of harmonics used in the Fourier basis, obtained for the G3T kinematics in the case of the CLOSED-curve (upper plot) and the OPEN-curve (lower plot) guidance-reference $\boldsymbol{q}_{3\mathrm{r}}(p)$.

guidance-reference[4]. Comparative results of the reconstruction accuracy are provided in Fig. 11 for the nS3T kinematics, and in Fig. 12 for the G3T kinematics.

[4] In the case of a prescribed backward reference motion along $\boldsymbol{q}_{3\mathrm{r}}(p)$, a numerical integration of (48) was performed using the backward p-flow ($\mathrm{d}p < 0$) to avoid the effects of instability in the joint-angles kinematics.

It is worth stressing that a precise execution of the guidance-references corresponding to the paths illustrated in Fig. 6, of rather medium complexity, is fairly demanding for the lengthy articulated vehicles (when related to the dimensions of the prescribed paths) characterized by parameters from Table 1. As a consequence, one shall expect a substantial reference-input effort required to follow the selected guidance-references, especially the OPEN curve.

Upon the obtained results one can formulate the following observations and remarks:

- The plots of reconstructed joint-references reveal their intricate evolution, in particular, for the guidance-reference corresponding to the OPEN curve. It is a consequence of the intentionally selected vehicles' lengths relative to moderate dimensions of the prescribed paths in a workspace, but it is also a consequence of the inherent nonminimum-phasiness of the N-trailer kinematics with off-axle hitching. The CLOSED path is simpler in execution, when compared to the OPEN one (mainly due to its larger dimensions and a smaller maximal absolute curvature), and leads to the reconstructed joint-references not exceeding the range of ± 1 rad. Practically acceptable accuracy of a reconstruction of the joint-references for the CLOSED path requires also a smaller number of harmonics in a Fourier basis. Although the OPEN path is much more difficult to follow by so long vehicles, the proposed reconstruction method found an admissible solution also in this difficult case.
- The reconstructed joint-references are periodic as a consequence of the postulate (39). By forcing this property, one is able to ensure satisfaction of the anti-jackknife admissibility condition C4 (observe the obtained reference longitudinal velocities $v_{i\mathrm{r}}(p)$ which are of the same sign for all $p \in [0, 1]$). On the other hand, imposition of the postulate (39) seems to preclude a flexible optimization of the evolution of admissible joint-references.
- The results obtained for the both forward as well as backward motion strategy have been computed not observing any special qualitative differences. This fact reveals some kind of a symmetry of the proposed reconstruction methodology with respect to a reference motion strategy, despite possible significantly different properties of the N-trailer kinematics for the forward and backward motion conditions, [15].
- By increasing a number of harmonics used in the Fourier basis, one gradually improves a reconstruction accuracy (at the points of sampling) observed by the decreasing values of cost K_1. A resultant accuracy with respect to n_{h} obtained in a task space (reflected by the values of costs K_2 and K_3) is improving up to some small but non-zero level. It is probably caused mainly by the unavoidable numerical integration errors accumulated when solving (48). However, under conditions of the addressed numerical examples, one may agree that usage of $n_{\mathrm{h}} \geq 200$ harmonics allows obtaining accuracy levels acceptable in most (if not all) practical tasks defined for the articulated vehicles of dimensions comparable to those from Table 1.

All the computations have been conducted in the Matlab R2015b environment. The source Matlab files, allowing one to reproduce the numerical results presented in this section (also for other kinematics studied in Section 2.4) for the closed-curve output-reference, are publicly available in [33].

6. Conclusions

The reconstruction method presented in the paper allows one to implement the reference signals generator for the whole configuration and for the input of the N-trailer vehicles in the case when the output-reference (in the form of a reference motion determined for a guidance segment) is *prescribed*. The method is

universal, thus it can be used in the reference generators for the trajectory-tracking and path-following tasks, and can be applied to any N-trailer kinematics with an arbitrary number of trailers and with arbitrary types of hitching used in a vehicle's chain (that is, for the nSNT, GNT, and SNT kinematics). It is worth emphasizing that the joint-references reconstructed upon the proposed method are determined in a continuous p-domain.

The inversion problem still remains open to some extent for the N-trailers. It is not known how to effectively find (if exist) the admissible joint-references satisfying the anti-jackknife condition C4 for the more general case where the postulate (39) is removed – see the case D in Fig. 4. A possible way to address this problem is to define it as a corresponding CCTOCP (see Remark 10) and search for an optimal solution by employing a direct collocation NLP. However, such an approach needs further investigations in view of possible difficulties with a convergence of NLP and its practical scalability with respect to a number of trailers and types of hitching. Furthermore, in the critical cases when the reconstructed joint-references are not acceptable from the practical point of view (e.g., if they violate mechanical limitations of a vehicle construction, or if they lead to unacceptably intricate reference motion for the whole vehicle chain), a possible remedy is a modification (or deformation, like in [16]) of a predefined output-reference in order to obtain a practically acceptable evolution of the subsequently reconstructed joint-references. However, finding an appropriate modification to the output-reference is a non-trivial task, whereas searching for this modification shifts, in fact, the inversion problem towards the motion planning.

Declaration of Competing Interest

The authors declare that they have no known competing financial interests or personal relationships that could have appeared to influence the work reported in this paper.

Acknowledgements

This work was supported in part by the National Science Centre, Poland, as the research grant No. 2016/21/B/ST7/02259, and in part by the research subvention No. 0211/SBAD/0120.

Appendix A

Partial derivatives of matrix $\boldsymbol{H}_j(\beta^*_{j\mathrm{r}}, \boldsymbol{u}_{j\mathrm{r}}, \dot{\boldsymbol{u}}_{j\mathrm{r}})$ take the following forms:

$$\frac{\partial \boldsymbol{H}_j}{\partial \beta^*_{j\mathrm{r}}} = \begin{bmatrix} 0 & 0 \\ L_j \mathrm{c}\beta^*_{j\mathrm{r}} & -\mathrm{s}\beta^*_{j\mathrm{r}} \end{bmatrix}, \tag{A.1}$$

$$\frac{\partial \boldsymbol{H}_j}{\partial \omega_{j\mathrm{r}}} = \begin{bmatrix} \frac{2L_j^3 \omega_{j\mathrm{r}} \dot{v}_{j\mathrm{r}}}{(v_{j\mathrm{r}}^2 + L_j^2 \omega_{j\mathrm{r}}^2)^2} & \frac{-2L_j^3 \omega_{j\mathrm{r}} \dot{\omega}_{j\mathrm{r}}}{(v_{j\mathrm{r}}^2 + L_j^2 \omega_{j\mathrm{r}}^2)^2} \\ 0 & 0 \end{bmatrix}, \tag{A.2}$$

$$\frac{\partial \boldsymbol{H}_j}{\partial v_{j\mathrm{r}}} = \begin{bmatrix} \frac{2L_j v_{j\mathrm{r}} \dot{v}_{j\mathrm{r}}}{(v_{j\mathrm{r}}^2 + L_j^2 \omega_{j\mathrm{r}}^2)^2} & \frac{-2L_j v_{j\mathrm{r}} \dot{\omega}_{j\mathrm{r}}}{(v_{j\mathrm{r}}^2 + L_j^2 \omega_{j\mathrm{r}}^2)^2} \\ 0 & 0 \end{bmatrix}, \tag{A.3}$$

$$\frac{\partial \boldsymbol{H}_j}{\partial \dot{\omega}_{j\mathrm{r}}} = \begin{bmatrix} 0 & \frac{L_j}{v_{j\mathrm{r}}^2 + L_j^2 \omega_{j\mathrm{r}}^2} \\ 0 & 0 \end{bmatrix}, \tag{A.4}$$

$$\frac{\partial \boldsymbol{H}_j}{\partial \dot{v}_{j\mathrm{r}}} = \begin{bmatrix} \frac{-L_j}{v_{j\mathrm{r}}^2 + L_j^2 \omega_{j\mathrm{r}}^2} & 0 \\ 0 & 0 \end{bmatrix}. \tag{A.5}$$

References

[1] E.L. Allgower, K. Georg, Numerical continuation methods. An introduction, Springer-Verlag, Berlin Heidelberg, 1990.
[2] C. Altafini, Some properties of the general n-trailer, Int. J. Control 74 (4) (2001) 409–424.
[3] M.D.D. Benedetto, P. Lucibello, Inversion of nonlinear time-varying systems, IEEE Trans. Automatic Control 38 (8) (1993) 1259–1264.
[4] M. Benosman, G.L. Vey, Stable inversion of SISO nonminimum phase linear systems through output planning: an experimental application to the one-link flexible manipulator, IEEE Trans. Cont. Sys. Technology 11 (4) (2003) 588–597.
[5] K. Bergman, D. Axehill, Combining homotopy methods and numerical optimal control to solve motion planning problems, in: 2018 IEEE Intell. Vehicles Symp., Changshu, China, 2018, pp. 347–354.
[6] K. Bergman, O. Ljungqvist, D. Axehill, Improved path planning by tightly combining lattice-based path planning and optimal control, in: IEEE Trans. Intell. Vehicles, 2020. DOI: 10.1109/TIV.2020.2991951 (early access)
[7] L. Biagiotti, C. Melchiorri, Trajectory Planning for Automatic Machines and Robots, Springer-Verlag, Berlin Heidelberg, 2008.
[8] L. Bushnell, B. Mirtich, A. Sahai, M. Secor, Off-tracking bounds for a car pulling trailers with kingpin hitching, in: Proc. of the 33rd Conference on Decision and Control, Lake Buena Vista, USA, 1994, pp. 2944–2949.
[9] A. Chelouah, Extensions of differential flat fields and Liouvillian systems, in: Proc. 36th CDC, San Diego, 1997, pp. 4268–4273.
[10] D. Chen, B. Paden, Stable inversion of nonlinear non-minimum phase systems, Int. J. Control 64 (1) (1996) 81–97.
[11] S. Devasia, D. Chen, B. Paden, Nonlinear inversion-based output tracking, IEEE Trans. Automatic Control 41 (7) (1996) 930–942.
[12] M. Diehl, S. Gros, Numerical Optimal Control (preliminary and incomplete draft), Online manuscript, 2017.
[13] A.W. Divelbiss, J.T. Wen, A path space approach to nonholonomic motion planning in the presence of obstacles, IEEE Trans. Robot. Autom. 13 (3) (1997a) 443–451.
[14] A.W. Divelbiss, J.T. Wen, Trajectory tracking control of a car-trailer system, IEEE Trans. Control Sys. Techn. 5 (3) (1997b) 269–278.
[15] M.M. Michałek, Non-minimum-phase property of N-trailer kinematics resulting from off-axle interconnections, International Journal of Control 86 (4) (2013) 740–758.
[16] K. Graichen, V. Hagenmeyer, M. Zeitz, A new approach to inversion-based feedforward control design for nonlinear systems, Automatica 41 (2005) 2033–2041.
[17] B. Houska, H.J. Ferreau, M. Diehl, ACADO toolkit - An open-source framework for automatic control and dynamic optimization, Optimal Control. Applications and Methods 32 (3) (2011) 298–312.
[18] A. Isidori, The zero dynamics of a nonlinear system: From the origin to the latest progresses of a long successful story, European Journal of Control 19 (5) (2013) 369–378.
[19] L. Jetto, V. Orsini, R. Romagnoli, Accurate output tracking for nonminimum phase nonhyperbolic and near nonhyperbolic systems, European Journal of Control 20 (6) (2014) 292–300.
[20] M. Kelly, An introduction to trajectory optimization: How to do your own direct collocation, SIAM Review 59 (4) (2017) 849–904.
[21] H.K. Khalil, Nonlinear systems. 3-Ed., Prentice-Hall, New Jersey, 2002.
[22] C. Knoll, K. Röbenack, Trajectory planning for a non-flat mechanical system using time-reversal symmetry, PAMM Proc. Appl. MAth. Mech. 11 (2011) 819–820.
[23] J.P. Laumond, Controllability of a multibody mobile robot, IEEE Trans. on Robotics and Automation 9 (6) (1993) 755–763.
[24] J. Levine, Analysis and Control of Nonlinear Systems. A Flatness-based Approach, Springer, Berlin Heidelberg, 2009.
[25] B. Li, T. Acarman, Y. Zhang, L. Zhang, C. Yaman, Q. Kong, Tractor-trailer vehicle trajectory planning in narrow environments with a progressively constrained optimal control approach, IEEE Trans. Intell. Vehicles (2019) 1–11. DOI: 10.1109/TIV.2019.2960943
[26] O. Ljungqvist, N. Evestedt, D. Axehill, M. Cirillo, H. Pettersson, A path planning and path-following control framework for a general 2-trailer with a car-like tractor, Journal of Field Robotics 36 (8) (2019) 1345–1377.
[27] M.M. Michałek, Cascade-like modular tracking controller for non-Standard N–Trailers, IEEE Trans. Cont. Syst. Technology 25 (2) (2017) 619–627.
[28] M.M. Michałek, Agile maneuvering with intelligent articulated vehicles: a control perspective, IFAC-PapersOnLine 52 (8) (2019) 458–473.
[29] M.M. Michałek, D. Pazderski, Computing the admissible reference state-trajectories for differentially non-flat kinematics of non-standard n-trailers, in: 2018 European Control Conference (ECC), Limassol, Cyprus, 2018, pp. 551–556.
[30] J. Minguez, F. Lamiraux, J.P. Laumond, Motion planning and obstacle avoidance, in: B. Siciliano, O. Khatib (Eds.), Springer handbook of robotics, Springer, 2008, pp. 827–852.
[31] M.J. van Nieuwstadt, R.M. Murray, Approximate trajectory generation for differentially flat systems with zero dynamics, in: Proc. 34th CDC, New Orleans, USA, 1995, pp. 4224–4230.
[32] J. Nocedal, S.J. Wright, Numerical optimization. Second Edition, Springer, 2006.
[33] D. Pazderski, M.M. Michałek, Reconstruction of the admissible joint-references for the N-trailer kinematics: the source Matlab files, 2020, ([Online] Available: https://doi.org/10.21227/h1h2-1486, IEEE Dataport). 10.21227/h1h2-1486.
[34] O.J.S. rdalen, Conversion of the kinematics of a car with n trailers into a

chained form, in: Proc. IEEE Int. Conf. on Robotics and Automation, Atlanta, USA, 1993, pp. 382–387.
[35] P. Rouchon, M. Fliess, J. Levine, P. Martin, Flatness, motion planning and trailer systems, in: Proc. 32nd Conf. Decision and Control, San Antonio, Texas, 1993, pp. 2700–2705.
[36] I.A. Shkolnikov, Y.B. Shtessel, Tracking in a class of nonminimum-phase systems with nonlinear internal dynamics via sliding mode control using method of system center, Automatica 38 (2002) 837–842.
[37] H. Sira-Ramrez, S.K. Agrawal, Differentially Flat Systems, CRC Press, Basel, 2004.
[38] O. von Stryk, Numerical solution of optimal control problems by direct collocation, in: R. Bulirsch, A. Miele, J. Stoer, K. Well (Eds.), Optimal Control – Calculus of Variations, Optimal Control Theory and Numerical Methods, 111, Birkhäuser, 1993, pp. 129–143.
[39] D.G. Taylor, S. Li, Stable inversion of continuous-time nonlinear systems by finite-difference methods, IEEE Trans. Automatic Control 47 (3) (2002) 537–542.
[40] K. Tchoń, I. Góral, Optimal motion planning for nonholonomic robotic systems, IFAC PapersOnLine 50 (1) (2017) 1910–1915.
[41] T.L. Vincent, W.J. Grantham, Nonlinear and optimal control systems, John Wiley & Sons, New York, 1997.
[42] Y. Yan-Qian, Others, Theory of limit cycles, American Mathematical Society, Providence, Rhode Island, 1986.